

**Biophysical Effects on U.S. Soybean Agroecosystems From  
Increasing Carbon Dioxide Concentration**

A THESIS  
SUBMITTED TO THE FACULTY OF THE GRADUATE SCHOOL  
OF THE UNIVERSITY OF MINNESOTA  
BY

JAROD J. BRYANT

IN PARTIAL FULFILLMENT OF THE REQUIREMENTS  
FOR THE DEGREE OF  
MASTER OF SCIENCE

TRACY TWINE

JANUARY 2011

Copyright

2011

Jarod J. Bryant ©  
All rights reserved

## Acknowledgments

I have been very fortunate to have this opportunity to be surrounded by such great scientists at the University of Minnesota. My advisor, Dr. Tracy Twine has provided me with great direction and support in both the writing process as well as the research that I have performed. She has been an excellent advisor as well as a personal mentor.

I would like to thank Dr. Andrew Leakey, Dr. Carl Bernacchi, Katie Richter and Andy Vanlooche for the data that they provided me from the SoyFACE experiment site. I would also like to thank Dr. Chris Kucharik for his help with the Agro-IBIS model. Without the data and support they provided none of the research would have been possible. They also provided me with useful insight on how to tackle some key research topics.

My lab members and office mates Keith Harding and Hong Xu have provided some personal support along the way as well. My former office mate, Mary Williams also provided me with a great deal of assistance. I would also like to thank all of the other graduate students in this department for their helpful critiques as well.

I would like to thank my committee members for their help during the writing and defense process. They provided very useful critiques of the thesis that helped to improve the thesis tremendously. Thanks to Dr. Peter Reich and Dr. Peter Snyder.

Finally I would like to thank Tracy Twine and Peter Snyder again. They have been very supportive and I am very fortunate to have gotten to know them. I have built both professional and personal relationships here that I hope to maintain for years to come.

## Abstract

An increase in the atmospheric concentration of carbon dioxide ( $[\text{CO}_2]$ ) is having an impact on many different aspects of the climate system including the surface energy budget. Several years of climatic and biological data have been collected for soybean, at the Soybean Free Air Concentration Enrichment (SoyFACE) site in Champaign, Illinois. Using these data I calibrated the Agro-IBIS (Integrated Biosphere Simulator, agricultural version) model to simulate the crop response to a  $\text{CO}_2$  enriched environment of 550 ppm and the ambient concentration of 375 ppm. Previously the model over predicted the  $\text{CO}_2$  fertilization effect at 550 ppm by overestimating the leaf area index (LAI). Realistic simulated LAI values are necessary for accurate simulation of transpiration, one component of the latent heat flux. I found that improving the phenology routine and adjusting the specific leaf area parameter results in a simulated LAI value that compares with the observations within the enriched and ambient environments. I also decreased the canopy conductance an additional 30% to simulate realistic latent heat flux values at 550 ppm. After validation at the SoyFACE site, I ran Agro-IBIS over the U.S. east of the Rocky Mountains with current and elevated  $\text{CO}_2$  concentrations. Here I show the impact that the response of soybean to elevated  $\text{CO}_2$  is expected to have on the latent and sensible heat fluxes across this domain with some areas expected to see a significant change to both of these terms of 10 – 20%. These predicted changes to the energy budget are important and need to be considered in future projections of ecosystem response to climate change.

# Table of Contents

## Table of Contents

<b>Acknowledgments</b> .....	<b>i</b>
<b>Abstract</b> .....	<b>ii</b>
<b>List of Tables</b> .....	<b>v</b>
<b>List of Figures</b> .....	<b>vi</b>
<b>List of Abbreviations</b> .....	<b>ix</b>
<b>1. Introduction</b> .....	<b>1</b>
<b>2. Literature Review</b> .....	<b>2</b>
2.1 Plant Physiological Response.....	2
2.2 Surface Energy Budget.....	4
2.3 Modeling Studies .....	6
<b>3. Methods</b> .....	<b>7</b>
3.1 Agro-IBIS Model Description .....	8
3.2 Site Description.....	9
3.3 Model parameterization and inputs .....	11
3.5 Model Evaluation .....	13
3.6 Model Runs at SoyFACE .....	15
3.7 Regional Model Runs.....	16
<b>4. Results</b> .....	<b>16</b>
<b>4.1 Model Improvements and Calibration at Ambient [CO<sub>2</sub>]: SoyFACE</b> .....	<b>16</b>
4.1.1 Assimilation.....	16
4.1.2 Stomatal Conductance .....	17
4.1.3 LAI.....	17
4.1.4 Energy Budget.....	20
<b>4.4 Model Improvement and Calibration at Elevated [CO<sub>2</sub>]: SoyFACE</b> .....	<b>20</b>
4.4.1 Assimilation.....	20
4.4.2 LAI.....	20
4.4.3 Water Vapor Conductance and Energy Budget.....	21
4.4.4 Dry Mass .....	21
<b>4.5 Future Scenarios - Regional Simulations</b> .....	<b>22</b>
4.5.1 LAI.....	22
4.5.2 Surface Energy Budget.....	22
<b>5. Discussion</b> .....	<b>23</b>
<b>6. Conclusions</b> .....	<b>25</b>
Future Research.....	26
<b>TABLES</b> .....	<b>28</b>
<b>FIGURES</b> .....	<b>30</b>

<b>Bibliography</b> .....	<b>50</b>
<b>Appendix I</b> .....	<b>54</b>
<b>Rosemount and Bondville Evaluation</b> .....	<b>54</b>
Bondville, IL.....	54
Rosemount, MN.....	55
<b>Results of the Model Evaluation at Ambient [CO<sub>2</sub>]: Ameriflux Sites</b> .....	<b>56</b>
4.3.1 LAI.....	56
4.3.2 Net Ecosystem Exchange.....	57
4.3.3 Energy Budget.....	58
<b>TABLES A1</b> .....	<b>60</b>
<b>FIGURES A1</b> .....	<b>61</b>
<b>Appendix II</b> .....	<b>65</b>
<b>Soil Carbon Simulations</b> .....	<b>65</b>
<b>Results of Soil Carbon Simulations</b> .....	<b>66</b>
<b>TABLES A2</b> .....	<b>68</b>
<b>FIGURES A2</b> .....	<b>69</b>

## List of Tables

<b>Table 1.</b> Key Agro-IBIS parameterizations altered in this study.....	28
<b>Table 2.</b> The validation data sources used in this study.....	28
<b>Table 3.</b> Initial and final carbon allocation parameters that determine the amount of carbon allocated to the different parts of the plant.....	29
<b>Table 4.</b> Model Energy Budget Errors for Ambient Conditions at SoyFACE. Errors were calculated using hourly mean values.....	29
<b>Table 5.</b> Model Energy Budget Errors for Elevated Conditions at SoyFACE. Errors were calculated using hourly mean values.....	29
<b>Table A1.1.</b> Mean Annual and Summer (June-August) Errors of Surface Energy Budget terms ( $\text{MJ m}^{-2}$ ) for the Rosemount and Bondville sites. Annual $R_{\text{net}}$ and G Errors for the Bondville site were calculated using 341 out of 366 days in 2004 and 325 of the 365 days in 2006. For the Rosemount site the annual $R_{\text{net}}$ and G errors were calculated using all days.....	60
<b>Table A2.1.</b> The descriptions of the accelerated carbon simulations.....	68

## List of Figures

<b>Figure 1.</b> Schematic of the Agro-IBIS model that includes modules for land surface physics, vegetation phenology and dynamics, below-ground biogeochemistry, crop management, and solute transport. Adapted from Kucharik (2003).....	30
<b>Figure 2.</b> Agro-IBIS grid cell showing the two distinct vegetation canopies, soil layers, snow layers, snow and water layers, and variables simulated at each time step. ....	30
<b>Figure 3.</b> Soybean maturity groups across the continental U.S. (Adapted from Zhang et al. 2007) .....	31
<b>Figure 4.</b> Fraction cover of soybean across the modeled U.S. domain (Donner and Kucharik 2003). .....	31
<b>Figure 5.</b> Observed and simulated assimilation rates for select days (2002-2004, and 2007) at the SoyFACE site prior to any modifications.....	32
<b>Figure 6.</b> Observed and simulated assimilation rates at ambient conditions for select days (2002-2004, and 2007) at the SoyFACE site.....	32
<b>Figure 7.</b> Scatter plot of observed versus simulated assimilation rates, before and after modification of temperature correction functions in Agro-IBIS for select days (2002-2004, and 2007) at the SoyFACE site.....	33
<b>Figure 8.</b> Observed and simulated stomatal conductance at ambient conditions for select days (2002-2004, and 2007) at the SoyFACE site.....	33
<b>Figure 9.</b> Scatter plot of observed versus simulated stomatal conductance for ambient conditions for select days (2002-2004, and 2007) at the SoyFACE site.....	34
<b>Figure 10.</b> Observed and simulated Intercellular CO <sub>2</sub> Concentration at ambient conditions for select days (2002-04, and 2007) at the SoyFACE site.....	34
<b>Figure 11.</b> Scatter plot of observed versus simulated Intercellular CO <sub>2</sub> Concentration for select days (2002-2004, and 2007) at the SoyFACE site.....	35
<b>Figure 12.</b> Simulated Leaf Area Index (LAI) from January 2002 to December 2007 for three simulations. The Original Code simulation uses the original parameters listed in Table 1 and Table 3. The Original Code with initial 0.1 LAI uses all the same parameters as the Original Code simulation but sets the initial LAI after emergence to 0.1 m <sup>2</sup> m <sup>-2</sup> instead of the default 0.01 m <sup>2</sup> m <sup>-2</sup> . The Original Code with initial 0.1 LAI and modified carbon allocation fractions uses the same parameters as the previous runs but contains the modifications that allows carbon allocation based on photoperiod. The Final code simulation contains all of the improvements.....	35
<b>Figure 13.</b> Observed Growing Degree-Days at SoyFACE for the years 2002 and 2004.	36
<b>Figure 14.</b> Simulated leaf fraction carbon allocation (aleaf) using a GDD of 1550 at SoyFACE site. ....	36
<b>Figure 15.</b> Ratio of Growing Degree-Days since planting divided by the heating units required to begin grain fill for 2002 and 2004 at the SoyFACE site.....	37



<b>Figure 16.</b> Simulated leaf fraction carbon allocation at the SoyFACE site using the observed GDD to maturity for 2002 and 2004. New fleaf is the new functions developed and old fleaf is using the old functions but using the observed GDD to maturity. ....	37
<b>Figure 17.</b> Calculated specific leaf area index (SLA) values using observed leaf dry mass and observed leaf area index measurements from the SoyFACE site. Only years 2002, 2004 and 2005 are plotted, however averaged values were calculated from all growing seasons available.....	38
<b>Figure 18.</b> Time series of model and observed dry mass values at the SoyFACE site for ambient conditions (2002-07). Data from 2003 were excluded due to crop damage from a hail storm. ....	38
<b>Figure 19.</b> SoyFACE LAI comparison showing the model’s performace prior to and after modifications (2002 and 2004 – 2007). ....	39
<b>Figure 20.</b> Time series of average daily values of the surface energy budget at ambient conditions at the SoyFACE site (2002). ....	39
<b>Figure 21.</b> Scatter plot of observed versus simulated assimilation rates for ambient and elevated conditions for select days (2002-2004, and 2007) at the SoyFACE site....	40
<b>Figure 22.</b> Observed and simulated intercellular CO <sub>2</sub> concentration at elevated conditions (2002-2004, and 2007) at the SoyFACE site. ....	40
<b>Figure 23.</b> SoyFACE simulated and observed LAI at ambient and elevated conditions for 2002-2007. ....	41
<b>Figure 24.</b> Scatter plot of observed versus simulated LAI for ambient and elevated conditions at the SoyFACE site (2002 and 2004 – 2007).....	41
<b>Figure 25.</b> Scatter plot of observed and simulated stomatal conductance for elevated conditions (2002 – 2004, and 2007) at the SoyFACE site.....	42
<b>Figure 26.</b> Obsereved and simulated stomatal conductance at elevated conditions (2002-2004, and 2007) at the SoyFACE site.....	42
<b>Figure 27.</b> Average daily values of the surface energy budget (2002) at elevated conditions. ....	43
<b>Figure 28.</b> Observed and simulated change in the latent heat flux (550 ppm – 375 ppm; 2002, 2004, 2005 and 2006). Significant at (p<0.05). ....	43
<b>Figure 29.</b> Observed and simulated change in the sensible heat flux (550 ppm – 375 ppm; 2002, 2004, 2005 and 2006) Significant at (p<0.05). ....	44
<b>Figure 30.</b> Time series of model and observed dry mass values at the SoyFACE site for elevated conditions (2002-07). Data from 2003 were excluded due to crop damage from a hail storm. ....	44
<b>Figure 31.</b> Simulated mean August LAI (m <sup>2</sup> m <sup>-2</sup> ) for 1953-2002. ....	45
<b>Figure 32.</b> Simulated difference in mean August LAI (m <sup>2</sup> m <sup>-2</sup> ; 550 ppm – ambient) for 1953 – 2002.....	45
<b>Figure 33.</b> Simulated annual mean Latent Heat Flux (W m <sup>-2</sup> ) for 1953-2002. ....	46
<b>Figure 34.</b> Simulated difference in annual mean latent heat flux (W m <sup>-2</sup> ; 550 ppm – ambient) for 1953 – 2002.....	46
<b>Figure 35.</b> Simulated mean August Latent Heat Flux (W m <sup>-2</sup> ) for 1953-2002. ....	47
<b>Figure 36.</b> Simulated difference in mean August latent heat flux (W m <sup>-2</sup> ; 550 ppm – ambient) for 1953 – 2002.....	47

<b>Figure 37.</b> Simulated annual mean sensible heat flux ( $\text{W m}^{-2}$ ) for 1953-2002.....	48
<b>Figure 38.</b> Simulated mean August sensible heat flux ( $\text{W m}^{-2}$ ) for 1953-2002.....	48
<b>Figure 39.</b> Simulated difference in annual mean sensible heat flux ( $\text{W m}^{-2}$ ; 550 ppm – ambient) for 1953 – 2002.....	49
<b>Figure 40.</b> Simulated difference in mean August sensible heat flux ( $\text{W m}^{-2}$ ; 550 ppm – ambient) for 1953 – 2002.....	49
<b>Figure A1.1.</b> Plot of simulated LAI for Rosemount MN from 2004 to 2006. Three different maturity groups were simulated to test the maturity group functions.....	61
<b>Figure A1.2.</b> Simulated LAI for Bondville IL from 2002 to 2006. Three maturity groups were simulated to test the maturity group functions.....	61
<b>Figure A1.3.</b> Scatter plot of observed versus simulated LAI for all three sites (SoyFACE – 2002 and 2004 to 2007; Rosemount – 2004 to 2006; Bondville – 2002 to 2006)..	62
<b>Figure A1.4.</b> Average monthly NEE for the Bondville IL site for 2004-2006.....	62
<b>Figure A1.5.</b> Average monthly NEE for Rosemount MN for 2004-2006.....	63
<b>Figure A1.6.</b> Time series of the averaged monthly surface energy budget (2004 – 2006) for the Rosemount MN Site.....	63
<b>Figure A1.7.</b> Time series of the averaged monthly surface energy budget (2004 – 2006) for the Bondville IL Site. Observations for the months of April and June are not shown because of many missing data points in the net radiation observations.....	64
<b>Figure A2.1.</b> Simulated soil carbon at SoyFACE from 1750-2001 (Urbana, IL,; 40° 02' N, 88° 14' W, 228 m above sea level).....	69

## List of Abbreviations

A – assimilation rate  
Agro-IBIS – Integrated Biosphere Simulator, agricultural version  
Aleaf – leaf allocation fraction  
aroot – the fraction of carbon allocated to the roots  
arootf – allocation of carbon at the end of the growing season to the roots  
arooti – initial carbon allocated to the roots  
[CO<sub>2</sub>] – atmospheric carbon dioxide  
adnpp – average daily net primary production  
bfact – coefficient in LAI curve  
R<sup>2</sup> – coefficient of determination  
DGVM – Dynamic Global Vegetation Model  
fleaf – the fraction of aboveground carbon going to the leaf  
fleafi – initial fraction of aboveground carbon allocated to the leaves  
G – soil heat flux  
g – stomatal conductance  
GCM – global climate model  
GDD – growing degree days  
grnfill – fraction of GDD (to reach maturity) for grain fill initiation  
H – sensible heat flux  
LE – latent heat flux  
LAI – leaf area index  
V<sub>max</sub> – maximum RuBP saturated rate of carboxylation  
K<sub>o</sub> – Michaelis-Menten constant for O<sub>2</sub>  
NCAR – National Center for Atmospheric Research  
NCEP – National Centers for Environmental Prediction  
NEE – net ecosystem exchange  
NARCCAP – North American Regional Climate Change Assessment Program  
PAR – photosynthetically active radiation  
pft – plant functional type  
R<sub>net</sub> – net radiation  
SoyFACE – Soybean Free Air Concentration Enrichment  
SLA – specific leaf area  
SURFRAD – Surface Radiation Network  
astem – the fraction of carbon that is allocated to the stem  
CRU05 – University of East Anglia Climate Research Unit datasets  
WUE – water use efficiency  
WRF – Weather Research and Forecasting model

## 1. Introduction

Atmospheric carbon dioxide ( $[\text{CO}_2]$ ) concentrations are predicted to continue rising with a concentration of 550 ppm expected by 2050 (Pacala and Socolow, 2004). Crops with C3 photosynthetic pathways respond to this change by increasing their photosynthetic rate and by decreasing their stomatal conductance (Ainsworth and Rogers, 2007). Soybean (*Glycine max*) is a major C3 crop grown in the United States. This crop was grown on an estimated 30.22 million ha in 2008-09—second only to corn in acreage (USDA, 2010). Because of the large acreage of soybean, future management of this crop relies on an increased understanding of the biophysical impacts of increasing atmospheric  $[\text{CO}_2]$ .

Biophysical impacts of increased atmospheric  $[\text{CO}_2]$  on soybean include decreased stomatal conductance (Bernacchi et al., 2006), increased leaf area index (LAI) and longer growing periods due to the continued addition of leaves later into the growing season than ambient conditions (Dermody et al., 2006). This reduction in stomatal conductance offsets the increase in LAI and leads to a decrease in evapotranspiration (Bernacchi et al., 2007), which is usually the second largest term in the energy budget over a growing soybean canopy. Other terms of the energy budget, such as net radiation and sensible heat flux, can also be altered as a result of these impacts. For example, increased LAI can lead to a decrease in net radiation while the decreased evapotranspiration leads to an increase in the sensible heat flux (Bernacchi et al., 2007). Accurately simulating the vegetation response to the impacts of elevated  $[\text{CO}_2]$  along with subsequent effects on the regional energy budget will advance understanding of the

main drivers in atmospheric general circulation models (GCMs) that simulate future climate scenarios (Sellers et al., 1997).

The Soybean Free Air Concentration Enrichment (SoyFACE) site is an advanced research facility that allows scientists to grow crops in an open environment with an elevated [CO<sub>2</sub>] concentration. This research is important because soybean is a major crop in the U.S. and these biophysical impacts of increased [CO<sub>2</sub>] will likely affect much of the Midwest. I used an agro-ecosystem model to take the results from the SoyFACE site and scale them up to the U.S. domain so that I could examine the regional impacts of increased [CO<sub>2</sub>] on the U.S. soybean ecosystem.

## **2. Literature Review**

### **2.1 Plant Physiological Response**

Atmospheric carbon dioxide [CO<sub>2</sub>] concentrations are expected to rise to 550 ppm by 2050 (Pacala and Socolow, 2004). Plants respond to increasing levels of [CO<sub>2</sub>] through increased photosynthesis and reduced stomatal conductance (Bernacchi et al., 2006; Ainsworth and Rogers, 2007). Stomatal conductance continues to decrease as [CO<sub>2</sub>] increases with no changes in stomatal density (Ainsworth and Rogers 2007). The reduction in stomatal conductance and increased photosynthesis are two fundamental processes that are responsible for many different changes to the plants, their associated ecosystems, and ultimately, the climate (Long et al., 2004).

In C3 plants, the stomatal pores allow for the mesophyll cells to be in direct contact with air from the atmosphere. These mesophyll cells contain Ribulose-1, 5-Bisphosphate Carboxylase-Oxygenase (RuBisCO) enzymes needed for photosynthesis.

As atmospheric [CO<sub>2</sub>] concentrations rise, so does the CO<sub>2</sub> concentration inside the leaf. The increasing intercellular CO<sub>2</sub> concentration results in an increased photosynthetic rate by providing more carbon to the RuBisCO enzymes in the plant cells and by inhibiting the competing oxygenation reaction that leads to photorespiration (Long et al., 2004). This process continues until intercellular CO<sub>2</sub> reaches saturated levels. For C3 plants, CO<sub>2</sub>-saturation may not occur until ambient [CO<sub>2</sub>] levels reach 800 to 2000 ppm (Long et al., 2006).

In many chamber studies, C3 crop yields increased more than 13% (Long et al., 2006) with an increased [CO<sub>2</sub>] concentration of 550 ppm. The largest growth responses to elevated [CO<sub>2</sub>] were found to occur when the plants were moisture stressed (Kimball et al., 1993; Field et al., 1997; Arp et al., 1998; McMurtrie et al., 2008) and can be attributed to increased water use efficiency (WUE) as a result of decreased stomatal conductance (McMurtrie et al., 2008). With decreased transpiration, the plants were not as likely to incur water stress, which maintained the high photosynthetic rates over longer periods. Because of this effect, C3 plants are more likely to survive a drought in increased [CO<sub>2</sub>] environments than they are at current [CO<sub>2</sub>] levels.

Light-saturated soybean crops, at 25°C with a [CO<sub>2</sub>] concentration of 550 ppm, can result in a 31- 36% increase (Ainsworth and Rogers, 2007; Long et al., 2004) in plant photosynthesis. This increase in production rate was a result of increased photosynthesis per unit leaf area (Long et al., 2004). Increasing photosynthesis levels require plants to use more CO<sub>2</sub> to complete the photochemical reaction. In a [CO<sub>2</sub>] enriched environment, C3 plants assimilate 13% more carbon (Long et al., 2004).

In C4 plants, RuBisCO is found in bundle sheath cells in which CO<sub>2</sub> is concentrated to three to six times atmospheric [CO<sub>2</sub>] (von Caemmerer and Furbank, 2003). This concentration is sufficient to saturate the RuBisCO and would likely limit the plant's ability to increase their uptake of CO<sub>2</sub> with rising atmospheric [CO<sub>2</sub>] concentrations (Long et al., 2006). However, increased [CO<sub>2</sub>] does lead to reduced stomatal conductance in C4 crops, which increases the WUE. This increased water use could lead to enhanced photosynthetic rates when the crop is water limited (Long et al., 2006).

## 2.2 Surface Energy Budget

Because of the reduction in stomatal conductance with increased [CO<sub>2</sub>], plants transpire less water vapor into the atmosphere. This lower transpiration rate causes the temperature near the surface of the plants to rise due to decreased evaporative cooling, which is the energy that is absorbed from the environment to evaporate the water (Long et al., 2006). Increased leaf and canopy temperatures affect plants that rely on evaporative cooling to regulate their leaf temperatures. This decrease in the latent heat flux could significantly alter the energy budget over areas where C3 and C4 crops dominate the landscape.

Changes to the surface energy budget due to the biophysical impact of elevated [CO<sub>2</sub>] could have a large influence on the climate in the Midwest (Sellers et al., 1997). The surface energy budget is defined as

$$R_{\text{net}} = H + LE + G \quad (1)$$

where  $R_{\text{net}}$  is the net radiation at the surface (balance of incoming and outgoing radiation),  $H$  is the sensible heat flux (heat energy transferred between the surface and air when there is a difference in temperature between them),  $LE$  is the latent heat flux (energy given or taken up by evaporation, transpiration or condensation), and  $G$  is the soil heat flux. This equation follows the fundamental conservation of energy principle and neglects the energy that is consumed during photosynthesis and energy stored in vegetation. With increased  $[\text{CO}_2]$  the magnitude of these terms may be altered but the energy must be conserved.

The energy budget will be impacted by the physiological changes that increased  $[\text{CO}_2]$  will have on soybean growth. At the SoyFACE site, the midday stomatal conductance was found to decrease by 16% (Bernacchi et al., 2006), while LAI increased on average by 10% (Dermody et al., 2006) at a  $[\text{CO}_2]$  concentration of 550 ppm. This reduction in stomatal conductance led to an average decrease in evapotranspiration of 12% despite the increase in LAI (Bernacchi et al., 2007). Because plants transpire less water vapor in a  $[\text{CO}_2]$ -enriched environment there is a decrease in  $LE$ . At the SoyFACE site, instantaneous canopy temperatures in the enriched environment were found to increase by over  $2^\circ\text{C}$  but on average they increase by  $0.2^\circ\text{C}$  (Bernacchi et al., 2007). The canopy temperatures can be over  $0.5^\circ\text{C}$  higher around midday and early afternoon resulting in increases in  $H$  of  $40 \text{ W m}^{-2}$  (Bernacchi et al., 2007). During the growing season the elevated  $[\text{CO}_2]$  also results in a decrease in  $R_{\text{net}}$ , though it is not statistically significant for all years (Bernacchi et al., 2007).



### 2.3 Modeling Studies

Since the 1990s research has been focused on the possible regional impacts of increased  $[\text{CO}_2]$  on the surface energy budget (Pollard and Thompson, 1995; Ramankutty et al., 2006). However, these studies have dealt with crops as if they were grasslands, despite the differences in phenology and physiology. For example, crops and grasses are very different in terms of their transpiration rates. Crops are also heavily managed ecosystems that cannot be properly represented by simulating the growth and development of unmanaged grasses. These key differences can result in significantly different simulations of the water and energy balances over the year.

Studies that have linked GCMs and Dynamic Global Vegetation Models (DGVMs) found increases in simulated LAI with increasing  $[\text{CO}_2]$  (Cramer et al., 2001). However, these studies did not use observations to determine whether or not the results were realistic. To date no modeling study has used observations from the SoyFACE site to evaluate the performance of models at both the leaf-level scale as well as the canopy level scale. These studies relied on flux tower measurements for validation, which were only available at ambient  $[\text{CO}_2]$  conditions. In this study I used physiological and phenological observations taken at ambient and enriched  $[\text{CO}_2]$  concentrations at the SoyFACE site to evaluate the performance of simulated soybean in the Agro-IBIS model. This is an improvement over previous studies that either did not evaluate the performance of the model or validated the model using observations from chambers.

The SoyFACE experimental site allows scientists to examine the impacts that increased  $[\text{CO}_2]$  will have on crops grown in the U.S. The SoyFACE site has eliminated several limitations that were seen by growing the crops in greenhouses or open-top

chambers, such as the “chamber effect” and the “pot effect” (Long et al., 2004). The chamber effect arises because of an artificial increase in temperature due to restricted air movement. The pot effect arises when the plants encounter a barrier, which has been shown to limit soybean response to increased [CO<sub>2</sub>] by decreasing yields as much as four times values found in open field plots (Ainsworth et al., 2002). Because of the availability of measurements from the SoyFACE site for validation, this modeling study is an improvement from other studies (Rosenzweig and Parry, 1994). This study increases the confidence in the model’s ability to simulate crop development in a [CO<sub>2</sub>] enriched world.

### **3. Methods**

First I evaluated and improved representation of the response of soybean to ambient [CO<sub>2</sub>] concentrations using measurements made at the SoyFACE facility. Measurements of stomatal conductance, assimilation rates and intercellular CO<sub>2</sub> concentrations were used to test the leaf-level processes of the model. I also used LAI and energy budget measurements at SoyFACE to evaluate the model’s canopy scale performance. The model was also evaluated at two Ameriflux sites—Rosemount, MN and Bondville, IL—under ambient conditions (see Appendix I). I tested and calibrated Agro-IBIS at SoyFACE at a [CO<sub>2</sub>] concentration of 550 ppm. I then ran the model over the U.S. and examined the predicted biophysical impacts of increased [CO<sub>2</sub>] on U.S. soybean agroecosystems.

### 3.1 Agro-IBIS Model Description

Agro-IBIS is a process-based ecosystem model that simulates the growth of managed and natural vegetation and their interaction with the environment (Kucharik and Brye, 2003). Agro-IBIS was developed by adapting the Integrated Biosphere Simulator (IBIS; Foley et al., 1996; Kucharik et al., 2000; Fig. 1) to simulate the major crop systems of the U.S. Agro-IBIS includes 11 soil layers of varying thickness to a depth of 2.5 meters, an upper and lower vegetation canopy, and three snow layers (Kucharik et al., 2000; Fig. 2). The model can represent 17 plant functional types (pfts) including trees, shrubs, C3 and C4 grasses and crops. The crops include corn, soybean, and spring and winter wheat. Each of the 11 soil layers is characterized with one of 11 soil texture classes with corresponding physical attributes. The model runs at an hourly or half-hourly time step, which is forced using several different atmospheric data sets.

Canopy exchange processes are controlled by physiologically based formulations of leaf-level photosynthesis (Farquhar et al., 1980), stomatal conductance, (Collatz et al., 1991) and respiration (Ryan, 1991). LAI is calculated independently for each PFT within the canopy. The LAI is calculated at each time step using accumulated leaf tissue carbon multiplied by the pft's specific leaf area (SLA; Table 1). Canopy and land surface processes are based on differences in assimilation rates and stomatal conductance between C3 and C4 crops. Crop phenology (i.e., emergence, budburst, grain fill, maturity and senescence) is simulated using summations of growing degree days (GDD) after the date of planting. Agro-IBIS simulates crop yield, harvest index, soil carbon, dry matter production, root dynamics and nitrogen dynamics (Kucharik and Brye, 2003). Planting dates in Agro-IBIS are prescribed or estimated based on a GDD threshold. The total

evapotranspiration from the land surface is treated as the sum of three water vapor fluxes: evaporation from the soil or snow surface, evaporation of water intercepted by vegetation canopies, and plant canopy transpiration. Canopy transpiration is a function of canopy conductance, LAI and the specific humidity gradient between the canopy and atmosphere.

The model has been validated at the Mead, Nebraska AmeriFlux site with three years of biometric data, soil temperature and moisture data, and eddy covariance measurements for a corn-soybean rotation (Kucharik and Twine, 2007). Agro-IBIS has also been used to look at the yield and nitrate losses for Wisconsin maize (Kucharik and Brye, 2003) and the impacts of maize grown for biofuel on nitrogen export by the Mississippi River (Donner and Kucharik, 2008). The interannual variability in maize yield across the U.S. Corn Belt has also been examined with the model (Kucharik, 2003). This model has been used to examine the potential rates of carbon sequestration in the Midwest (Kucharik et al., 2000), and the flow of nitrogen pools in the Mississippi River basin (Donner et al., 2002; Donner and Kucharik, 2003).

### **3.2 Site Description**

The SoyFACE project site is located within a 32 ha field at the University of Illinois South Farms in Champaign, IL (40.25N, 88.25W, 230 m a.s.l.) The soil series is Drummer-Flanagan (fine-silty, mixed, mesic Typic Endoaquoll), which is typically very deep and formed from loess and silt parent material deposited on the till and outwash plains (Bernacchi et al., 2006). The site has been continuously cultivated for over 100 years. Soybean and corn are each planted in half of the field and are rotated annually. After harvest the crop is chopped with a mower and tilled with a rip chisel. Prior to

planting in the spring, the fields are cultivated with a single-rip cultivator. No fertilizer is applied before planting the soybean (Morgan et al., 2005).

SoyFACE plots are circular (20 meters in diameter or 314 m<sup>2</sup> in area) and are lined with pipes around the border that release CO<sub>2</sub> gas (Hamilton et al., 2005). The pipes extend vertically so that gas is released throughout the plant canopy as well as just above the canopy. The concentration of CO<sub>2</sub> is controlled by a computer adjustment system that measures the wind direction and magnitude as well as the concentration at the center of the plot. With these measurements the computer then adjusts where in the circle to release the gas and how much of the gas is to be released (Rogers et al., 2004).

The computer controlled CO<sub>2</sub> levels are relatively constant with the one-minute average concentration ranging about 10% of the targeted level for 90% of the time (Long et al., 2004). A disadvantage of the system is the natural variability of the wind. This causes the concentrations on the downwind side to be slightly lower and the windward side to be slightly higher, while the center remains closer to the targeted level (Long et al., 2004). This treatment method was shown to have no bias in concentration levels after averaging over the entire growing season (Leavitt et al., 1996).

At SoyFACE, canopy-level and leaf-level processes are measured. Leaf-level measurements of the maximum RuBP saturated rate of carboxylation ( $V_{\max}$ ), stomatal conductance, assimilation rates and intercellular CO<sub>2</sub> concentrations are used in this study. The canopy-level measurements used in this study include LAI, dry mass values, phenological stages, and surface energy budget components. Observations of LAI were collected periodically throughout the growing season with 14 measurements in 2002, 16 in 2004, 15 in 2005, 5 in 2006, 7 in 2007 and 9 in 2008. Daily average values of all

components of the energy budget are compared with simulated values. The components of the surface energy budget were estimated at the SoyFACE site using the residual energy budget method. This method uses the measured  $R_{\text{net}}$ ,  $H$ , and  $G$  to calculate the  $LE$  as the residual of the energy balance equation (Eq. 1; Bernacchi et al., 2007; Hickman et al., 2010).

### 3.3 Model parameterization and inputs

Agro-IBIS requires a single soil texture profile at each model grid cell. The Flanagan soil profile was used to run the model at the SoyFACE site. The  $[CO_2]$  concentration was set to 375 ppm (referred to hereafter as ambient) for the ambient simulations and 550 ppm (referred to hereafter as elevated) for the elevated simulations to match the SoyFACE growing conditions.

Meteorological input datasets were compiled for the SoyFACE site. The measurements include solar radiation, air temperature, precipitation, wind speed, and humidity. Precipitation data was collected from Willard Airport (40.04N, -88.27W; approximately 24 km from the site) while all other forcing variables were collected from the nearest Surface Radiation Network (SURFRAD) site (40.05N, -88.37W; approximately 23 km from the site) for 2002-2008 (Table 2).

Two climate driver datasets were used for the regional runs. These driver datasets were created by combining 1961-1990 climatological mean values and 1901-2002 monthly mean climate data as given by the University of East Anglia Climate Research Unit datasets (CRU05; New et al., 1999; Mitchell and Jones, 2005) along with anomalies of meteorological data for 1948-2002 from the National Centers for Environmental Prediction-National Center for Atmospheric Research (NCEP / NCAR) reanalysis dataset

(Kalnay et al., 1996; Kistler et al., 2001). Using these data, Agro-IBIS calculates hourly values empirically using diurnal relationships of meteorological variables (Campbell and Norman, 1998).

Agro-IBIS requires many different parameters for all the equations. The GDD requirements used in the initial runs were determined by estimating the amount of GDD required to reach maturity using observed peak LAI values and observed temperatures at each site. The maximum LAI parameter limits the amount of carbon that is allocated to the leaf. This was originally set at a value of 6.0 but was changed to 10.0 to allow the model to simulate LAI without an artificial limit. The SLA is used to calculate the LAI using the average daily net primary production (adnpp) and the allocation fraction (aleaf). Prior to this study, the  $V_{\max}$  parameter for soybean was set at a value of  $45 \mu\text{mol CO}_2 \text{m}^{-2} \text{s}^{-1}$ . The  $V_{\max}$  value was lowered to  $40.5 \mu\text{mol CO}_2 \text{m}^{-2} \text{s}^{-1}$  to match observed values at SoyFACE from the growing seasons of 2001 and 2002 (Bernacchi et al., 2006). The same value is used for the elevated runs because the calculated average values are very close for both ambient and elevated  $[\text{CO}_2]$  conditions. The crop growth respiration coefficient (the fraction of carbon that is respired to the atmosphere) is set at 30% according to (Amthor, 1984).

To represent the range of varieties of soybean grown across the U.S. a soybean maturity group map (Fig. 3) was used to assign a maturity group hybrid to each grid cell for the regional runs (Zhang, 2007). For the SoyFACE model runs, a maturity group 3 was used to simulate plant development to fit the hybrid planted at the site (Pioneer 93B15).

### 3.5 Model Evaluation

Several key variables were used to evaluate the simulation of phenology, assimilation, LAI and NPP (Table 1). The LAI provides information on the amount of carbon that is being assimilated and converted to leaf biomass. This variable can thus be useful for model validation with biased values indicating low crop productivity and poor growing conditions, or limitations in the model algorithms. An overestimation of LAI can indicate an underestimation of stresses on the plants environment. The timing of the onset of leaf development, called leaf out, affects transpiration and surface albedo due to the leaves having a lower albedo than the bare soil. Agro-IBIS calculates the LAI daily at each grid cell as follows

$$lai(i) = lai(i - 1) + (SLA * aleaf * \max(0.0, adnpp)) \quad (2)$$

where  $i$  is the time index and  $lai(i-1)$  is the previous day's LAI. The  $adnpp$  value is calculated by scaling up the leaf-level gross assimilation to the canopy scale and then subtracting the carbon that is respired by the leaves, stems and roots.

Agro-IBIS calculates  $aleaf$  daily as follows

$$aleaf = \max(0.0, (1.0 - aroot) * fleaf) \quad (3)$$

where  $aroot$  is the fraction of carbon allocated to the roots and  $fleaf$  is the fraction of aboveground carbon going to the leaf. Both  $aroot$  and  $fleaf$  are functions of the ratio between GDD since planting ( $gddplant$ ) and a heating unit function of GDD to maturity ( $gddmaturity$ , Table 1.). The  $fleaf$  and  $aroot$  terms are calculated as follows

$$fleaf = fleafi * \frac{\exp(-bfact) - \exp(-bfact * \frac{gddplant}{grnfill * gddmaturity})}{\exp(-bfact) - 1} \quad (4)$$



$$aroot = \min(1.0, (arooti - (arooti - arootf) * \min(1.0, \frac{gddplant}{gddmaturity}))) \quad (5)$$

where the variables *fleafi* (initial fraction of aboveground carbon allocated to the leaves), *arooti* (initial carbon allocated to the roots), *arootf* (allocation of carbon at the end of the growing season to the roots), *bfact* (coefficient in LAI curve) and *grnfill* (fraction of GDD to maturity for grain fill initiation) are constants for each pft (Table 3).

The fraction of carbon that is allocated to the stem (*astem*) is calculated daily as the remainder of carbon after the carbon has been allocated to both the stem and leaf as

$$astem = 1.0 - aroot - aleaf \quad (6)$$

This equation is valid from emergence to the initiation of grain fill. At the initiation of grain fill, allocation to the leaves, stem and root is halted. After this point all of the carbon that is assimilated is allocated to the reproductive pools and the root and leaf biomass pools start to decline to represent the decay of leaves and roots.

To improve representation of the developmental stages a new soybean phenology routine was added to Agro-IBIS, which simulates phenology based on the combined response of soybean to temperature (measured as GDD) and photoperiod (Setiyono et al., 2007). Because of the addition of functions for maturity group, the number of GDDs required to reach maturity was no longer used to denote crop maturity. Carbon allocation functions were dependent on the GDD to reach maturity, therefore this dependency was removed and new carbon allocation fractions using observed temperatures during 2002 and 2004 were developed.

Agro-IBIS calculates leaf-level photosynthesis following Farquhar et al., (1980). These equations account for light-limited assimilation as well as Rubisco-limited

assimilation. To improve the environmental response of the model, new temperature response functions for Rubisco-limited assimilation from Bernacchi et al., (2001) were added.

Stomatal conductance is calculated as

$$g = m * \frac{A * h}{C} + b \quad (7)$$

where A is the assimilation rate, m (=9.0) and b (=0.01) are the slope and intercept for soybean, h is the leaf-level humidity and C is the leaf-level CO<sub>2</sub> concentration. Realistic stomatal conductance values are important to correctly simulate transpiration rates. Because the amount of water vapor that is transpired by the plants contributes a large fraction to the LE.

The coefficient of determination (R<sup>2</sup>) was used as a relative index of short timescale model performance. Simulated model errors were calculated in both absolute and relative terms (percentage) for the energy balance. Daily values were used for evaluating the energy budget performance.

### 3.6 Model Runs at SoyFACE

To examine the simulated impacts of increased [CO<sub>2</sub>] on soybean, two simulations were run for the SoyFACE site, one for ambient [CO<sub>2</sub>] conditions and one at elevated [CO<sub>2</sub>] conditions. Both runs used the same meteorological driving data and were run for the entire year for the period 2002-2008. Model simulations were run at an hourly time step. Natural vegetation was simulated at the site during model spin-up with the carbon acceleration procedure (See Appendix II) used for the period 1750-1889. Corn was simulated for 1889-2000, and soybean for 2001-2008.

### 3.7 Regional Model Runs

After testing and improving Agro-IBIS at the SoyFACE site the model was run over the U.S. east of the Rocky Mountains (49°45'N: 24°45'N, 106°45'W: 66°45'W) at a spatial resolution of 0.5° x 0.5°. Two simulations were performed, one for ambient [CO<sub>2</sub>] conditions and one for elevated [CO<sub>2</sub>] conditions. For both simulations natural vegetation was simulated with the accelerated soil carbon procedure from 1750-1889, corn was grown from 1889-1952, and soybean was grown from 1953-2002. To examine the impacts of increased [CO<sub>2</sub>] on soybean agroecosystems, grid cells were only included in the analysis if the fraction cover of soybean exceeded 10% (Fig. 4). The same climate forcing datasets were used for both simulations.

## 4. Results

### 4.1 Model Improvements and Calibration at Ambient [CO<sub>2</sub>]: SoyFACE

#### 4.1.1 Assimilation

Assimilation rates in the initial model run were underestimated, which led to low values for LAI compared to observations (Fig. 5). Modification of the Michaelis-Menten constant for O<sub>2</sub> (K<sub>o</sub>) and V<sub>max</sub> functions (Bernacchi et al., 2001) resulted in assimilation rates much closer to observations (Fig. 6). Overall, the regression between measured and simulated values yielded a slope of 1.38 and an intersect of 1.3831 using the default functions and a slope of 0.89 and an intersect of 0.8658 with the updated functions (Fig. 7). There is a low bias in simulated values in the middle of the day that occurs in both simulations (Fig. 5 and 6). This bias occurs because the model decreases the amount of photosynthetically active radiation (PAR) that is absorbed by the canopy in the middle of

the day. Because observed assimilation rates do not drop in the middle of clear days, this issue should be further analyzed.

#### 4.1.2 Stomatal Conductance

The model is able to simulate the overall diurnal variability of the stomatal conductance (Fig. 8) with reasonable accuracy (Fig. 9). The model slightly overestimates the stomatal conductance ( $R^2=0.55$ ), which leads to an underestimation of intercellular  $CO_2$  concentration from early morning to mid-afternoon, but it does well in the late afternoon (Fig. 10). This pattern can also be seen in Fig. 11, where lower observed concentrations occur during the day ( $R^2 = 0.65$ ).

#### 4.1.3 LAI

Simulated maximum LAI values are underestimated in the initial model run (Fig. 12). The model underestimated the maximum LAI value by an average of  $3.5 \text{ m}^2 \text{ m}^{-2}$  for the 2002, 2005, 2006 and 2007 growing season. In 2002 the model predicts a maximum LAI of  $2.6 \text{ m}^2 \text{ m}^{-2}$  while the measured value is  $6.7 \text{ m}^2 \text{ m}^{-2}$ , however the peak simulated LAI value in 2004 was close to observations. Seeds contain a small amount of energy that is expended when shoots break through the soil. To account for this energy, initial LAI values were subsequently set to  $0.1 \text{ m}^2 \text{ m}^{-2}$  at emergence (instead of  $0.01 \text{ m}^2 \text{ m}^{-2}$  in the initial model). With this stimulation, LAI reached values much closer to observations, however LAI is overestimated in all years except 2002 (Fig. 12).

The fraction of assimilated carbon that is allocated to different parts of the plant changes with the growth stage. In the initial model run, onset of growth stages occurred according to the fraction of the number of GDD needed to reach maturity. The years 2002 and 2004 had very different climates, with 2002 accumulating GDD faster than 2004

(Fig. 13). Observations show that soybean reached maturity at about the same time for both years however the model was not able to predict this because of the difference in the GDD between both years. Instead, the model simulated a higher leaf fraction allocation in 2004 versus 2002 because the development stage of the crop lasted longer with a slower accumulation of GDD (Fig. 14).

While the number of GDD accumulated at different rates in 2002 and 2004, it was found that the time dependent ratio of the number of GDD since planting and heating unit function ( $gdd_{plant} / hu_{grain}$ ) is linear and is conserved for both years (Fig. 15). The previous function of GDD was replaced with this ratio in order to produce similar allocation fractions in both years (Fig. 16). Because the relationship is conserved for both years, this method results in plants that will develop at the same rate in both years, which is validated by the observations. A similar method was used to replace the dependence of GDD in the root allocation fractions. These modifications resulted in simulated LAI values that were less variable than before, but the values were still overestimated as compared with observations (Fig. 12).

The overestimation in LAI is related to an overestimation in leaf dry mass. Comparisons with observations show that simulated leaf dry mass values are about twice the observed values. Assimilation rates validated with observations, however, LAI is also dependent on SLA and the allocation of carbon to leaves. SLA is a model parameter that varies by pft but is constant over time. Observed SLA is highly variable from year to year as well as within a growing season (Fig. 17). To simulate accurate peak values of LAI an average SLA value from emergence to peak LAI was used for all years ( $SLA = 77.5 \text{ m}^2 [\text{kg C}]^{-1}$ ).

Comparisons with observations show that the model was not accurately allocating carbon to the respective vegetation pools. To adjust this the values of  $f_{leaf}$  were lowered from 0.8 to 0.47. Also, the values used for  $a_{rooti}$  and  $a_{rootf}$  were increased from 0.25 to 0.35 (Table 3). According to the observations the plant did not stop the allocation of carbon to the stems at the initiation of grain fill like the model simulated. The allocation equations were adjusted to continue allocation to the stems and roots until ten days past the day that grain fill begins. This results in dry mass values close to observations.

After adjustments to the allocation fractions were made, the model simulates biomass values close to observations for all plant components (i.e., stem, leaves, grain, and root; Fig. 18). Grain has the largest biomass by weight, followed by stems, roots, and finally leaves. Root biomass observations were not made at SoyFACE. Over all growing seasons, the model predicts biomass within 23% for grain, 32.1% for stems, and 17.3% for leaves. Values less than  $25 \text{ g m}^{-2}$  were neglected in the error calculations because of the small magnitudes resulting in large percent errors. Because point observations of biomass capture the peak in biomass of each component, it was assumed that the maximum observation given in Figure 18 is the actual peak value. The model overestimates grain biomass in 2004, 2006, and 2007. The largest error of  $204.558 \text{ g m}^{-2}$  occurs in 2004. The model underestimates leaf biomass by  $44.08 \text{ g m}^{-2}$  in 2005 but is similar to observations for other years.

By fitting a 2nd degree polynomial to observed LAI measurements at SoyFACE, a new decline function was developed that initiates the decline of the LAI once maturity is reached. The addition of the new soybean phenology subroutine, the decline function, the changes made to the carbon allocation functions, and SLA values based on

observations, resulted in a significant improvement in the simulated LAI both in timing and magnitude (Fig. 12). The correlation between measured and observed values improved from an  $R^2$  of 0.25 to 0.88 (Fig. 19).

#### **4.1.4 Energy Budget**

The model reasonably simulates the energy budget at SoyFACE for ambient conditions (Fig. 20). Model errors over the growing season for the LE term were less than 19% (Table 4) and less than 11% for the  $R_{net}$  term. Errors for the H and G term were larger with errors ranging from 0.1 to 604% for the H term and 6.7 to 139.2% for the H term.

### **4.4 Model Improvement and Calibration at Elevated $[CO_2]$ : SoyFACE**

#### **4.4.1 Assimilation**

The model simulates an increase in assimilation with increased  $[CO_2]$  concentrations that corresponds to observations (Fig. 21). The linear trends for both of these simulations are very close to one another, meaning that the model only slightly overestimates the increase compared to ambient conditions ( $R^2$ :0.78; Fig. 21). Simulated intercellular  $CO_2$  also increases with increasing atmospheric  $[CO_2]$  (Fig. 22). The model generally underestimates the intercellular  $CO_2$  values (Fig. 11).

#### **4.4.2 LAI**

Observed values of LAI are not significantly greater at a  $[CO_2]$  concentration of 550 ppm than at ambient conditions (Bernacchi et al., 2006; Dermody et al., 2006); however, Agro-IBIS is too sensitive to the  $[CO_2]$  fertilization effect and overestimates the LAI for every year but these values are much closer than in previous versions of the model (Figs. 23 and 24).

#### 4.4.3 Water Vapor Conductance and Energy Budget

Simulated stomatal conductance has a larger bias and more scatter at elevated  $[\text{CO}_2]$  than at ambient conditions (Fig. 25). The model captures the diurnal variability well with a tendency to overestimate the stomatal conductance by  $0.08 \text{ mol C m}^{-2} \text{ s}^{-2}$  on average (Fig. 26). Simulated stomatal conductance is 13.8% lower at elevated  $[\text{CO}_2]$  conditions compared with ambient conditions. This decrease is similar to the 16% decrease found by Bernacchi et al. (2006); however, when leaf-level conductance is scaled to the canopy, it is 4.5% greater than observations. This bias appears to result from a limitation in the equation for the canopy conductance of water vapor flux, which is an empirical function of windspeed, canopy structure, and atmospheric stability. To obtain the correct magnitude of decreased transpiration rates with increased  $[\text{CO}_2]$  in the model, the canopy conductance is artificially reduced an additional 30% each time period.

With the canopy conductance adjustment, the model simulates the surface energy budget at 550 ppm  $[\text{CO}_2]$  closer to observations. LE (Fig. 27) is lowered significantly ( $p < 0.05$ ) with increased  $[\text{CO}_2]$  (Fig. 28). The daily averaged LE observations decreased by  $86.58 \text{ MJ m}^{-2}$  on average during the growing season for all years while the model simulates a decrease of  $65.98 \text{ MJ m}^{-2}$ . With this reduction in LE there is a significant ( $p < 0.05$ ) increase in H due to the reduction in evaporative cooling. At SoyFACE, observations of H increased by an average of  $86.77 \text{ MJ m}^{-2}$  and the model simulates an average increase of  $35.02 \text{ MJ m}^{-2}$  (Fig. 29).

#### 4.4.4 Dry Mass

At 550 ppm, the overestimation in assimilation by Agro-IBIS leads to overestimation in predicted biomass of grain in all years (30% error; Fig. 30). Stem biomass is overpredicted in 2002, 2004, and 2007 with an overall bias of 34.3%. The leaf



biomass pool is overpredicted in 2002 and 2007 and results in an overestimation of 41.6%. This is an area of the model that needs to be further evaluated.

#### **4.5 Future Scenarios - Regional Simulations**

To examine the biophysical impacts of increased [CO<sub>2</sub>] on U.S. soybean agroecosystems I ran the model over the U.S. east of the Rocky Mountains. I used the Agro-IBIS that was calibrated with data from SoyFACE and assumed that all soybean ecosystems will show the same response to elevated [CO<sub>2</sub>].

##### **4.5.1 LAI**

Peak LAI in most of the soybean-growing region (north of ~38°N) occurs in August. The average LAI for the month of August (1953-2002) at ambient [CO<sub>2</sub>] ranged from 1 to 4 m<sup>2</sup> m<sup>-2</sup> (Fig. 31). Increases in LAI between the ambient and 550 ppm runs were not statistically significant at p<0.05 (Fig. 32) for most locations. The grid cells with significant differences were on the borders of maturity groups.

##### **4.5.2 Surface Energy Budget**

Annual mean (1952-2002) LE values at ambient [CO<sub>2</sub>] range between 30 and 70 W m<sup>-2</sup> and decrease with increasing latitude across the domain (Fig. 33). Annual mean LE decreases at each grid cell as [CO<sub>2</sub>] increases from ambient to 550 ppm, but these decreases are not statistically significant at p<0.05 (Fig. 34). Values of LE at ambient [CO<sub>2</sub>] are highest across the Corn Belt region for the month of August (Fig. 35) as a result of the timing of peak LAI. August mean LE decreases by as much as 18 W m<sup>-2</sup> between the ambient and 550 ppm runs (Fig. 36). This decrease of 18 W m<sup>-2</sup> is equivalent to approximately 19 mm of water that is saved in the soil. Differences are statistically

significant ( $p < 0.05$ ) throughout most of Iowa, northern parts of Illinois and Indiana, and western Ohio.

Annual averages of H (1952-2002) at ambient  $[\text{CO}_2]$  are highest in western and southern areas of the domain (Fig. 37). The same pattern appears in the average values for the month of August (Fig. 38). Differences in annual mean H between the ambient  $[\text{CO}_2]$  and 550 ppm  $[\text{CO}_2]$  runs are not statistically significant (Fig. 39). The same areas that see a significant decrease in LE with increasing  $[\text{CO}_2]$  (Fig. 36) also see a significant increase in H ( $> 12 \text{ W m}^{-2}$ ; Fig. 40) for the month of August.

## 5. Discussion

The Agro-IBIS model accurately simulates the response of elevated  $[\text{CO}_2]$  on soybean agroecosystems if the correct parameters are used. Using an appropriate SLA value in the model is necessary to simulate accurate LAI and biomass pools. SLA observations are highly variable throughout the growing season as well as from year to year (Fig. 18). The default Agro-IBIS model, like many ecosystem models, uses a constant value for this parameter; however, using the average value of each growing season in the model results in better agreement of simulated LAI with observations for all but one year (results not shown). To improve the performance of the model, a relationship needs to be developed for the SLA parameter that is based on the growing conditions for each season.

Improvement to the simulation of LAI results in improvement of the biomass pools for ambient and elevated conditions because of the effect LAI has on canopy level assimilation; however, for elevated conditions the simulated values of the grain, leaf and

stem biomass were still overestimated. Preliminary analysis of this overestimation shows that it is related to an overestimation of the LAI from the beginning of grain production to senescence. Furthermore, the model does not simulate the leaves turning brown before falling off of the plant. This overestimation of green leaves on the plant causes the model to overestimate canopy assimilation.

Stomatal conductance is a key variable in canopy transpiration. If the model is able to correctly simulate stomatal conductance at both ambient and elevated  $[\text{CO}_2]$ , it should be able to simulate the correct transpiration values as well. In this study it was shown that the model was able to simulate stomatal conductance values close to observations for both ambient and elevated  $[\text{CO}_2]$  conditions. The model was also able to simulate the energy balance well at ambient  $[\text{CO}_2]$  conditions but the change from ambient to elevated  $[\text{CO}_2]$  conditions was not represented in the model. After several approaches to adjusting the function to scale transpiration from the leaf to canopy failed, an empirical scaling factor was added to the transpiration flux equation that reduced the canopy conductance by 30% for elevated conditions. This 30% decrease was added to the decrease of 16% that was already simulated by the model at both the leaf-level scale as well as the canopy level scale. While the model does simulate stomatal conductance values close to the observations made at the SoyFACE site this may not be representative of the canopy scale values. At the SoyFACE site the stomatal conductance measurements were made using the youngest fully expanded leaves. This could have led to a bias in the reported value that is not represented in the model simulations.

Although observations from SoyFACE increase the number of datasets with which we can test the Agro-IBIS model, the SoyFACE site does have some limitations.

One such limitation is that for the growing seasons used in this study there was no artificial heating of the plant environment to represent the expected warming to the ambient atmosphere. The SoyFACE measurements are still useful and provide useful information but the  $[\text{CO}_2]$  fertilization effect is likely overestimated at the site due to the lack of increased temperatures. Depending on the magnitude of increased temperatures the plant's assimilation rates could possibly be lowered because of increased heat stress.

Regional simulations indicate that increasing  $[\text{CO}_2]$  will significantly impact the surface energy budget across the U.S. by decreasing LE and increasing H, especially over the Corn Belt. A decrease in LE across the region could increase the surface air temperature as excess radiation is partitioned into H, and not LE, thus increasing the potential for heat stress on plants, animals, and humans during the summertime. A reduction in LE could also contribute to a change in precipitation as the flux of moisture to the atmosphere is reduced. These climatic changes may dramatically alter the environment and should be considered when evaluating projections of future climate change and their impacts on the biosphere.

## 6. Conclusions

In this study I have shown that the Agro-IBIS model is able to correctly simulate the impacts of increased  $[\text{CO}_2]$  on soybean and the resulting changes to the regional energy budget. These changes to the energy budget demonstrate how increasing  $[\text{CO}_2]$  will impact the crops grown in the U.S. and how those changes could alter the environment. There is a need to continually improve the representation of crops in GCMs so that we can fully understand how increasing  $[\text{CO}_2]$  will impact humans in the future.

Results from this study suggest that increasing levels of [CO<sub>2</sub>] will cause significant changes to the energy and water balance across regions where soybean is grown. Agro-IBIS simulates significant decreases in LE and significant increases in H across parts of the Midwest. These results were found only by adjusting the SLA to values measured at the SoyFACE site and by adjusting the transpiration flux equation. With the adjustment of SLA the model agreed with observations and did not simulate a significant increase in LAI.

Many changes were made to the Agro-IBIS model to improve the simulation of soybean growth and development at both ambient and elevated [CO<sub>2</sub>]. The main changes were the addition of a new soybean phenology subroutine, a new decline function for LAI, an improved temperature response functions for assimilation and stomatal conductance calculations, and the use of an SLA value based on measurements. More work is needed to improve the change in the canopy transpiration flux equation with increased [CO<sub>2</sub>]; however, this is not an active area of research at this time. The empirical canopy conductance function is based on limited numbers of field studies and depends on complex relationships between atmospheric stability, wind flow through the canopy, and canopy architecture.

### **Future Research**

With increased levels of atmospheric [CO<sub>2</sub>] global temperatures are predicted to rise and precipitation patterns will be altered. These two factors could have large impacts on the growth and development of soybean. Researchers at the SoyFACE site are conducting experiments to examine how soybean will grow in a warmer and drier environment, and an environment with elevated ozone concentrations. Future studies will

use Agro-IBIS to represent these impacts and to examine how these changes will alter the energy and water budgets across the U.S.

It would be useful to couple Agro-IBIS to a regional model such as the Weather Research and Forecasting Model (WRF) to examine how changes to the water and energy budget would interact with the atmosphere to impact precipitation patterns, cloud cover, surface roughness, the surface energy budget, and temperature. To simulate more accurate results all of this work would need to be completed for corn as well because of the high acreage on which corn is currently grown. To examine how the spatial patterns of climate change would impact the growth of soybean the additional use of the North American Regional Climate Change Assessment Program (NARCCAP) scenarios would be useful. The NARCCAP scenarios are developed by an international program with the goal to produce high spatial resolution climate change simulations of dynamically downscaled GCM simulations using regional climate models (<http://www.narccap.ucar.edu>).

Agriculture plays an important role not only in feeding the population but also in influencing regional climates. This research is important and advances our understanding of how increased [CO<sub>2</sub>] will impact the functioning of the Earth system now and in the future.

## TABLES

**Table 1.** Key Agro-IBIS parameterizations altered in this study.

	Original Code	First Run	Final Code (Ambient CO <sub>2</sub> )	Final Code (550 ppm)
GDD to physiological maturity (gddmaturity)	variable (user-specified)	1550	n/a	n/a
GDD to leaf emergence	variable (user-specified)	46.5	n/a	n/a
GDD to grain fill initiation	variable (user-specified)	1085	n/a	n/a
Maximum LAI (m <sup>2</sup> m <sup>-2</sup> )	6.0	10	10	10
Growth Respiration	0.3	0.3	0.3	0.3
V <sub>max</sub> at 15 °C (μmol CO <sub>2</sub> m <sup>-2</sup> s <sup>-1</sup> )	45	40.53	40.53	40.53
Specific leaf area (SLA; m <sup>2</sup> kg Carbon <sup>-1</sup> )	56.5	52.5	89.0	77.5

**Table 2.** The validation data sources used in this study.

Site	G <sub>s</sub>	A <sub>n</sub>	C <sub>i</sub>	LAI	Energy Fluxes	NEE	Meteorological Data
SoyFACE	Leakey Unpublished (2002-2004)	Leakey Unpublished (2002-2004)	Leakey (2002-2004; 06,07)	Dermody 2006 (2002); Dermody from A. Leakey (2004-05); Justin (2004-08)	Bernacchi	n/a	Andy VanLoocke
Rosemount, MN	n/a	n/a	n/a	PIs T. Griffis J. Baker	PIs T. Griffis J. Baker	PIs T. Griffis J. Baker	PIs T. Griffis J. Baker
Bondville, IL	n/a	n/a	n/a	PIs C. Bernacchi, S. Hollinger	PIs C. Bernacchi, S. Hollinger	PIs C. Bernacchi, S. Hollinger	PIs C. Bernacchi, S. Hollinger

**Table 3.** Initial and final carbon allocation parameters that determine the amount of carbon allocated to the different parts of the plant.

	fleafi	arooti	arootf	aleaff	astemf	bfact	grnfill
Original Values	0.8	0.25	0.25	0.05	0.25	-2.50	0.63
Final Values	0.47	0.35	0.35	0.05	0.25	-2.50	0.63

**Table 4.** Model Energy Budget Errors for Ambient Conditions at SoyFACE. Errors were calculated using hourly mean values ( $\text{MJ m}^{-2}$ ).

Year	$R_{\text{net}}$			Sensible Heat			Latent Heat			Ground Heat		
	Model	Observed	Error (%)	Model	Observed	Error (%)	Model	Observed	Error (%)	Model	Observed	Error (%)
2002	761.18	851.49	10.6	105.94	35.9	195.05	649.86	798.39	18.6	18.02	16.89	6.7
2004	702.98	709.59	0.9	128.60	130.26	0.1	564.14	571.80	0.1	18.03	7.54	139.2
2005	650.81	617.28	5.4	107.00	36.64	192.0	536.92	572.30	6.2	18.83	8.33	125.9
2006	654.08	684.22	4.4	102.03	14.50	604.0	543.34	658.01	17.4	20.18	11.71	72.3

**Table 5.** Model Energy Budget Errors for Elevated Conditions at SoyFACE. Errors were calculated using hourly mean values ( $\text{MJ m}^{-2}$ ).

Year	$R_{\text{net}}$			Sensible Heat			Latent Heat			Ground Heat		
	Model	Observed	Error (%)	Model	Observed	Error (%)	Model	Observed	Error (%)	Model	Observed	Error (%)
2002	794.49	833.91	4.7	160.85	120.38	33.6	622.12	703.09	11.5	20.45	9.05	126.1
2004	656.46	697.01	5.8	160.20	245.02	34.6	476.55	448.60	6.2	23.00	3.39	577.8
2005	613.46	617.82	0.7	132.50	87.63	51.2	468.22	523.41	10.5	21.34	6.77	215.0
2006	610.54	703.21	13.2	130.12	111.34	16.9	463.47	579.05	20.0	24.40	12.81	90.4



## FIGURES

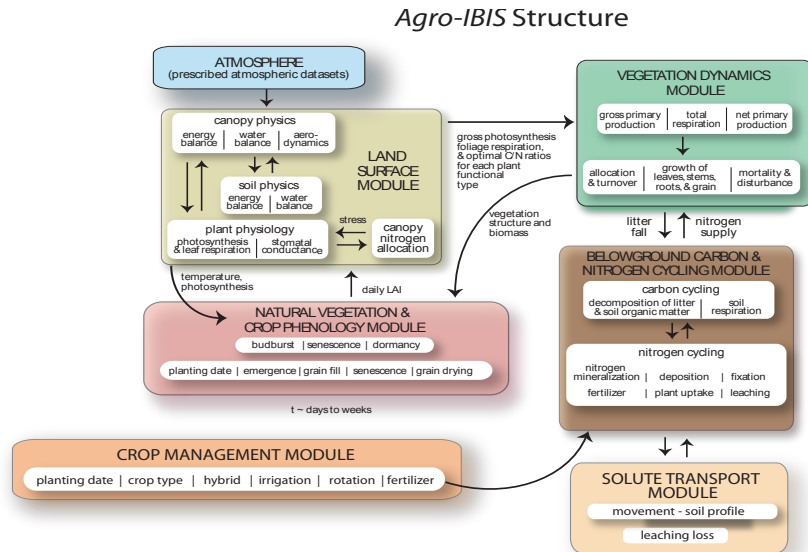


**Figure 1.** Schematic of the Agro-IBIS model that includes modules for land surface physics, vegetation phenology and dynamics, below-ground biogeochemistry, crop management, and solute transport. Adapted from Kucharik (2003).

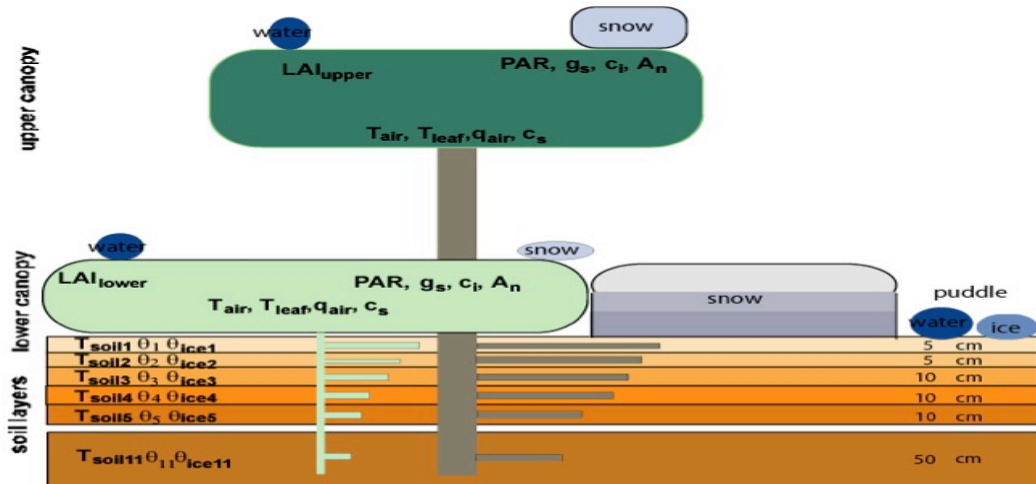


**Figure 2.** Agro-IBIS grid cell showing the two distinct vegetation canopies, soil layers, snow layers, snow and water layers, and variables simulated at each time step.

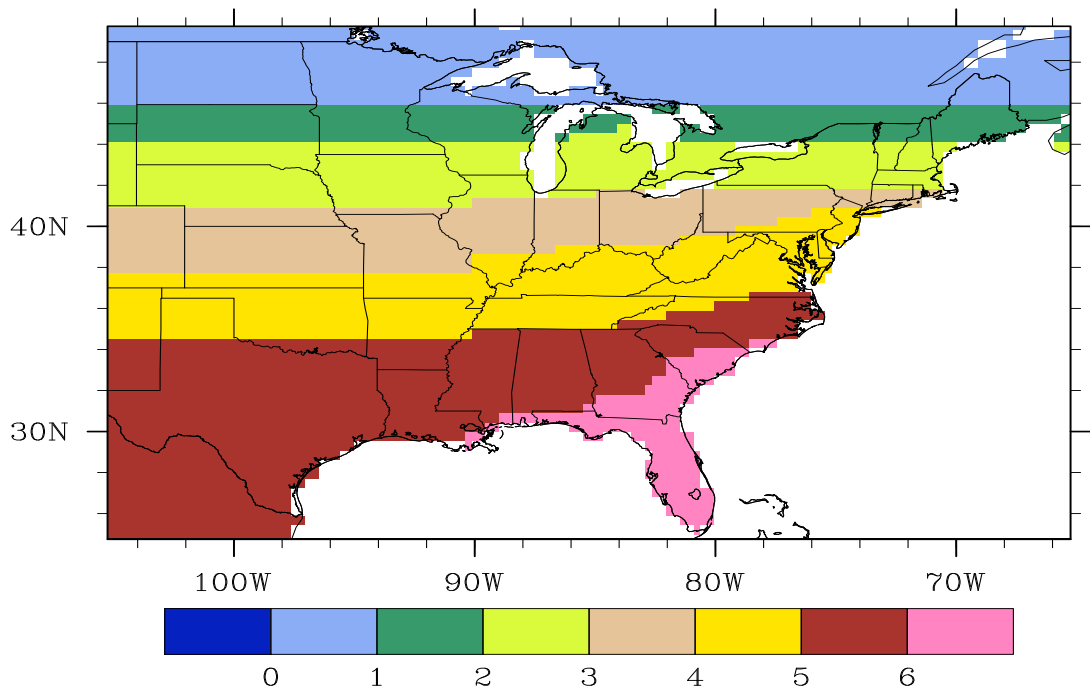


**Figure 3.** Soybean maturity groups across the continental U.S. (Adapted from Zhang et al. 2007)

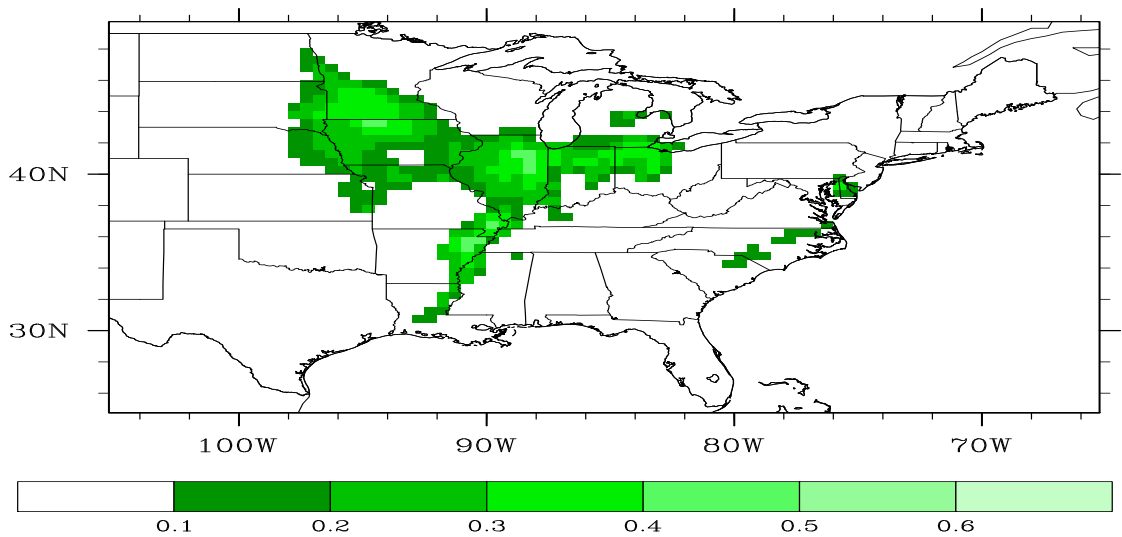


**Figure 4.** Fraction cover of soybean across the modeled U.S. domain (Donner and Kucharik 2003).

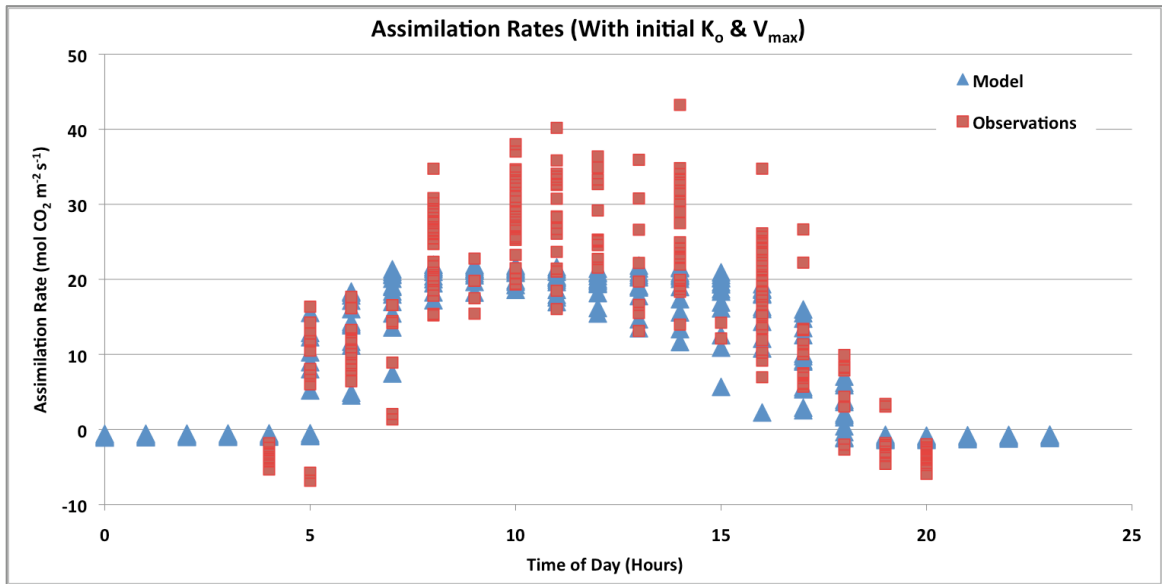


**Figure 5.** Observed and simulated assimilation rates for select days (2002-2004, and 2007) at the SoyFACE site prior to any modifications.

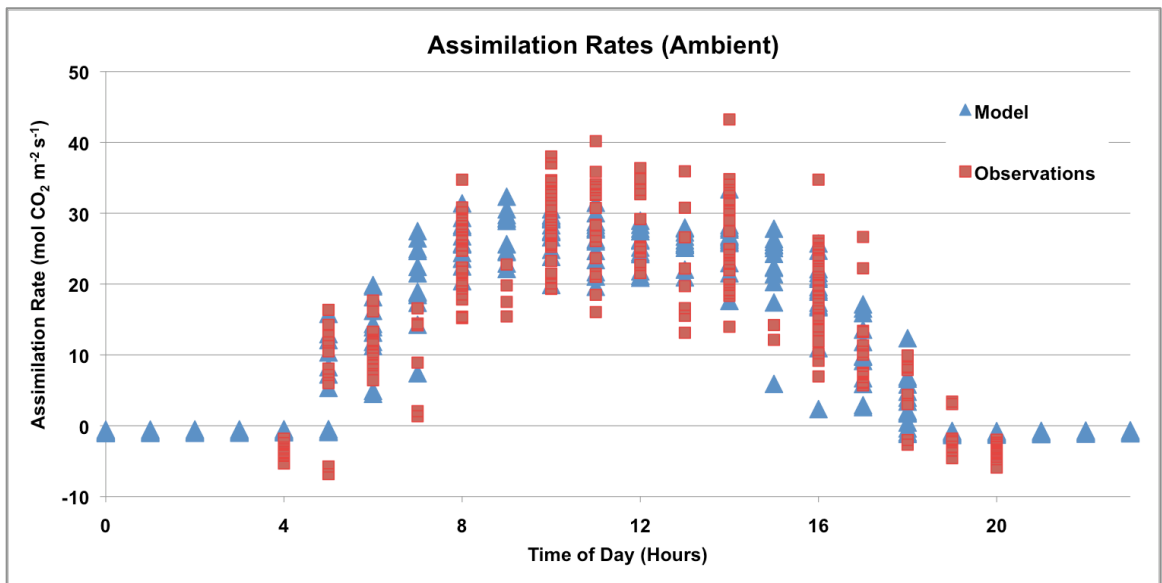


**Figure 6.** Observed and simulated assimilation rates at ambient conditions for select days (2002-2004, and 2007) at the SoyFACE site.

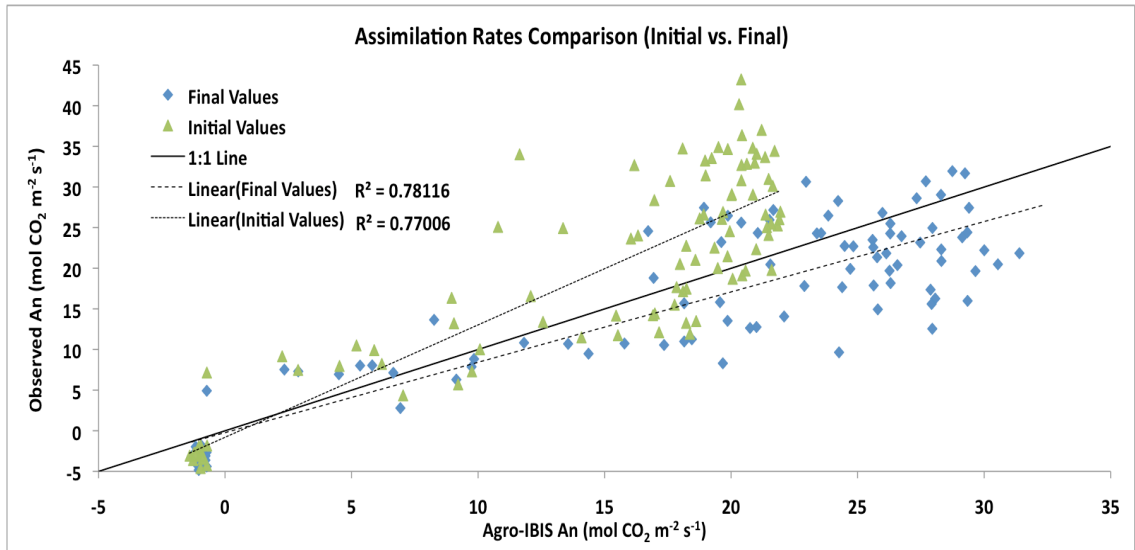


**Figure 7.** Scatter plot of observed versus simulated assimilation rates, before and after modification of temperature correction functions in Agro-IBIS for select days (2002-2004, and 2007) at the SoyFACE site.

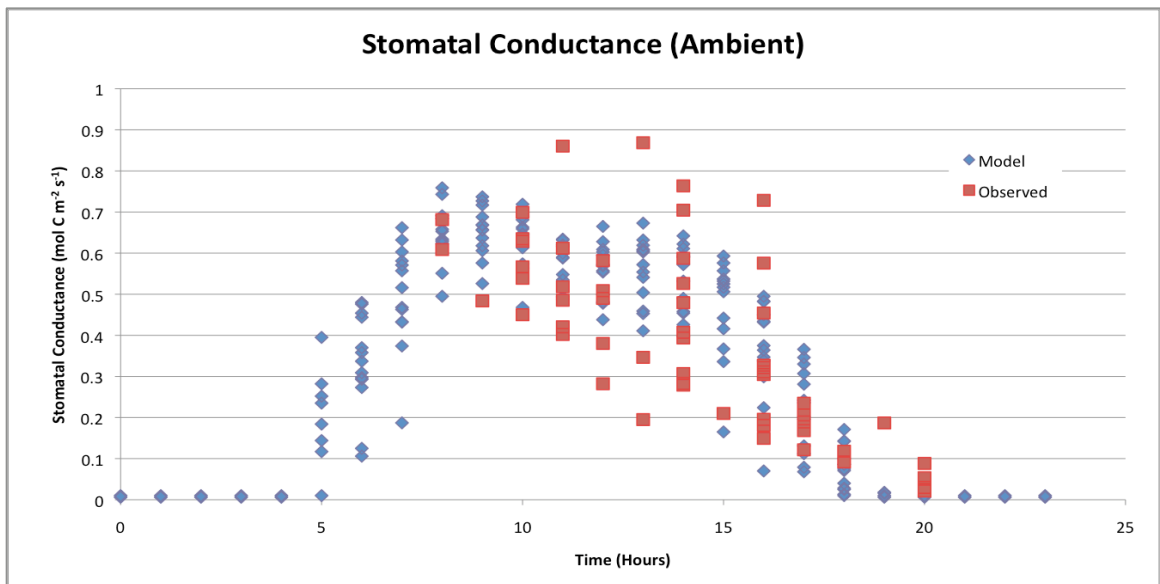


**Figure 8.** Observed and simulated stomatal conductance at ambient conditions for select days (2002-2004, and 2007) at the SoyFACE site.

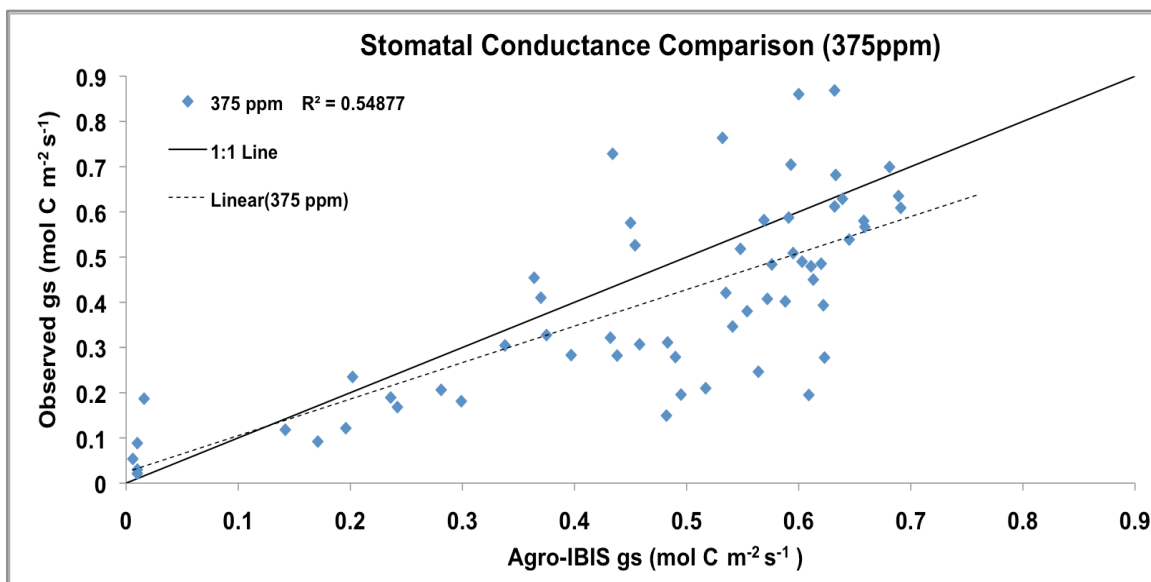


**Figure 9.** Scatter plot of observed versus simulated stomatal conductance for ambient conditions for select days (2002-2004, and 2007) at the SoyFACE site.

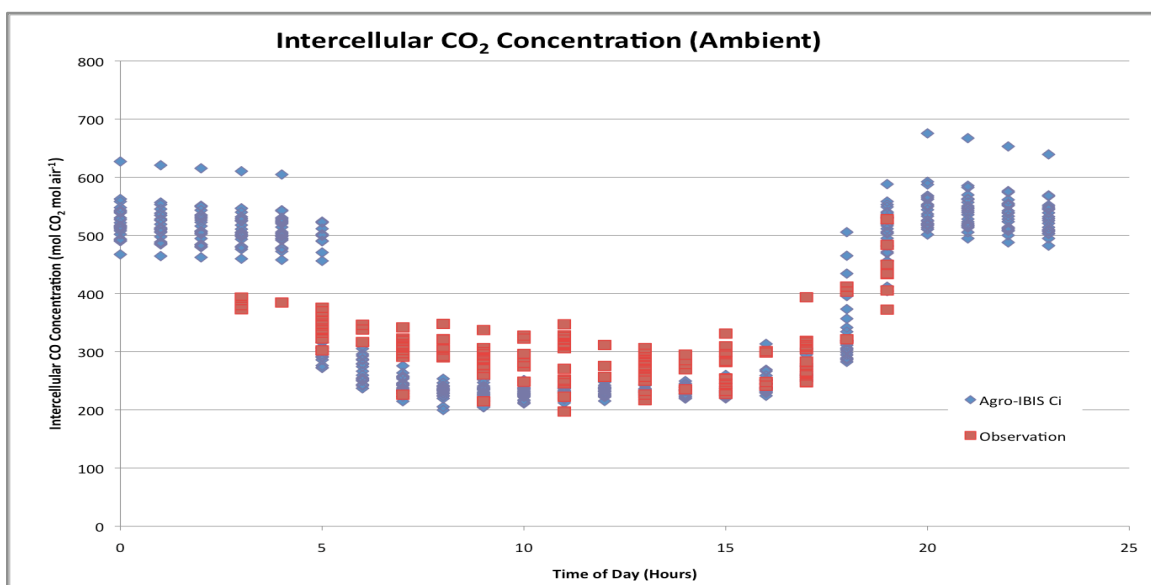


**Figure 10.** Observed and simulated Intercellular CO<sub>2</sub> Concentration at ambient conditions for select days (2002-04, and 2007) at the SoyFACE site.

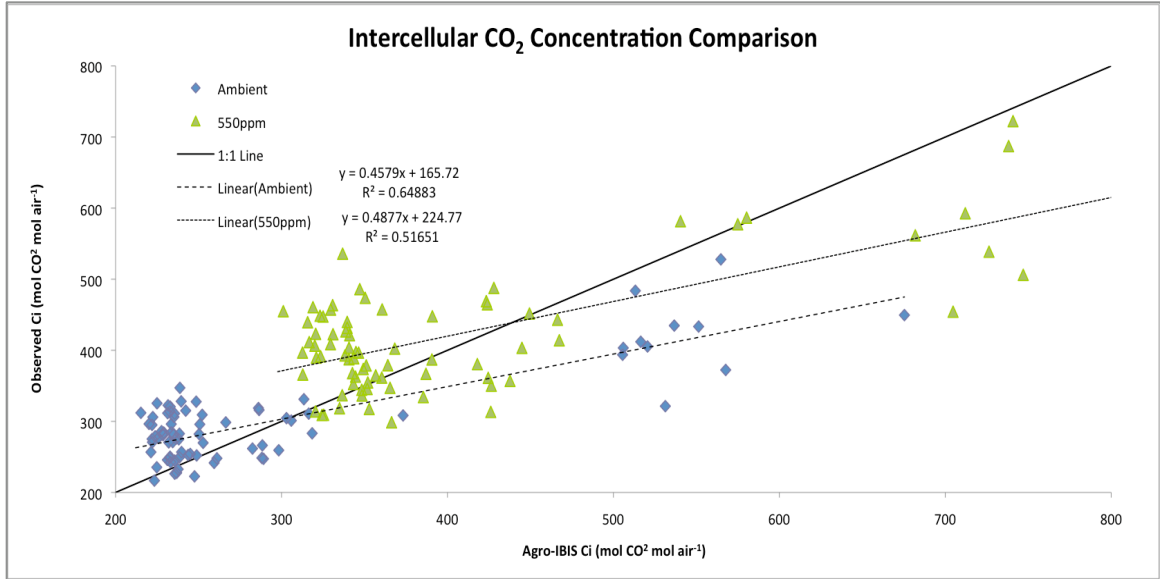


**Figure 11.** Scatter plot of observed versus simulated Intercellular CO<sub>2</sub> Concentration for select days (2002-2004, and 2007) at the SoyFACE site.

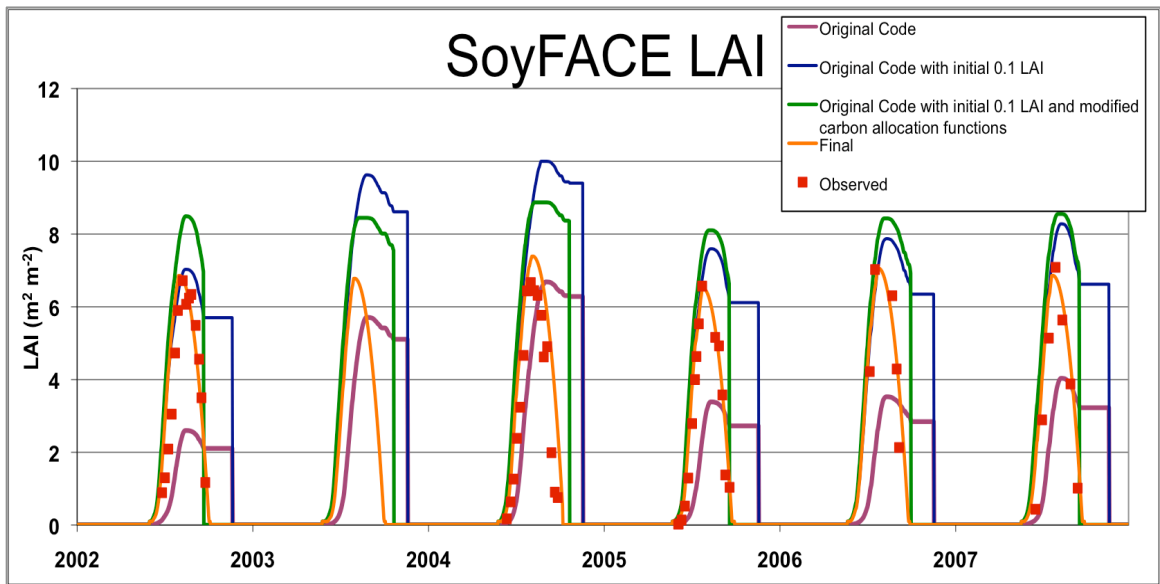


**Figure 12.** Simulated Leaf Area Index (LAI) from January 2002 to December 2007 for three simulations. The Original Code simulation uses the original parameters listed in Table 1 and Table 3. The Original Code with initial 0.1 LAI uses all the same parameters as the Original Code simulation but sets the initial LAI after emergence to 0.1 m<sup>2</sup>m<sup>-2</sup> instead of the default 0.01 m<sup>2</sup>m<sup>-2</sup>. The Original Code with initial 0.1 LAI and modified carbon allocation fractions uses the same parameters as the previous runs but contains the modifications that allows carbon allocation based on photoperiod. The Final code simulation contains all of the improvements.

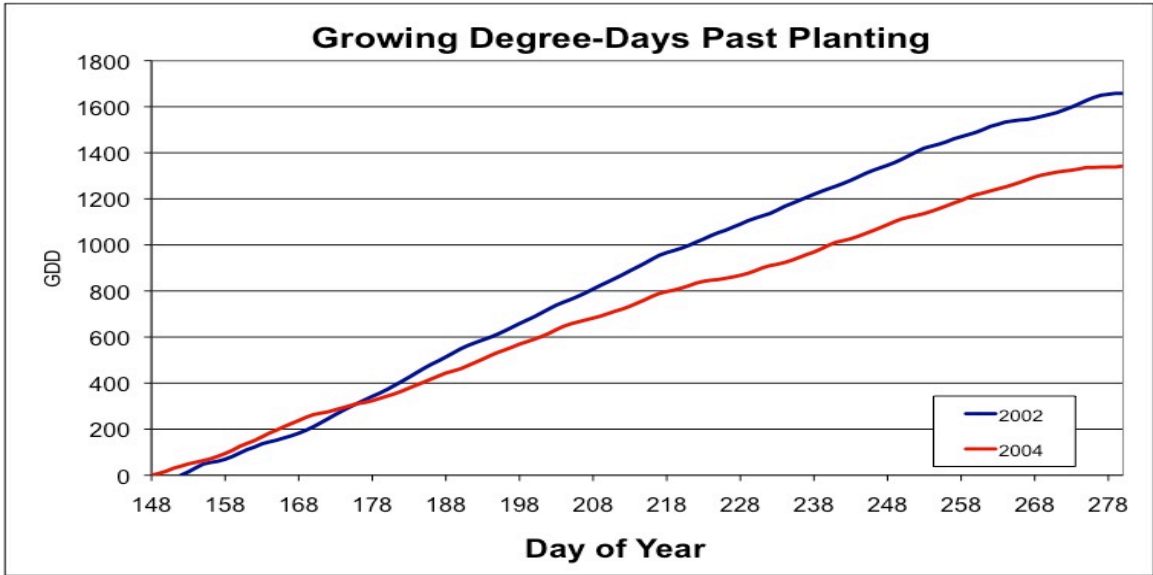


**Figure 13.** Observed Growing Degree-Days at SoyFACE for the years 2002 and 2004.

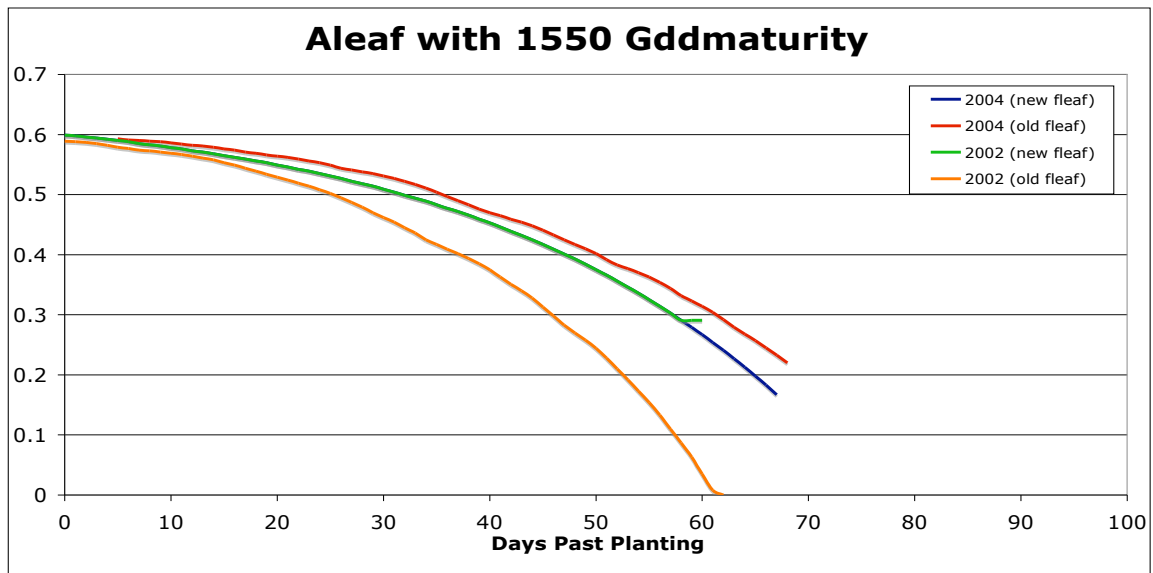


**Figure 14.** Simulated leaf fraction carbon allocation (aleaf) using a GDD of 1550 at SoyFACE site.

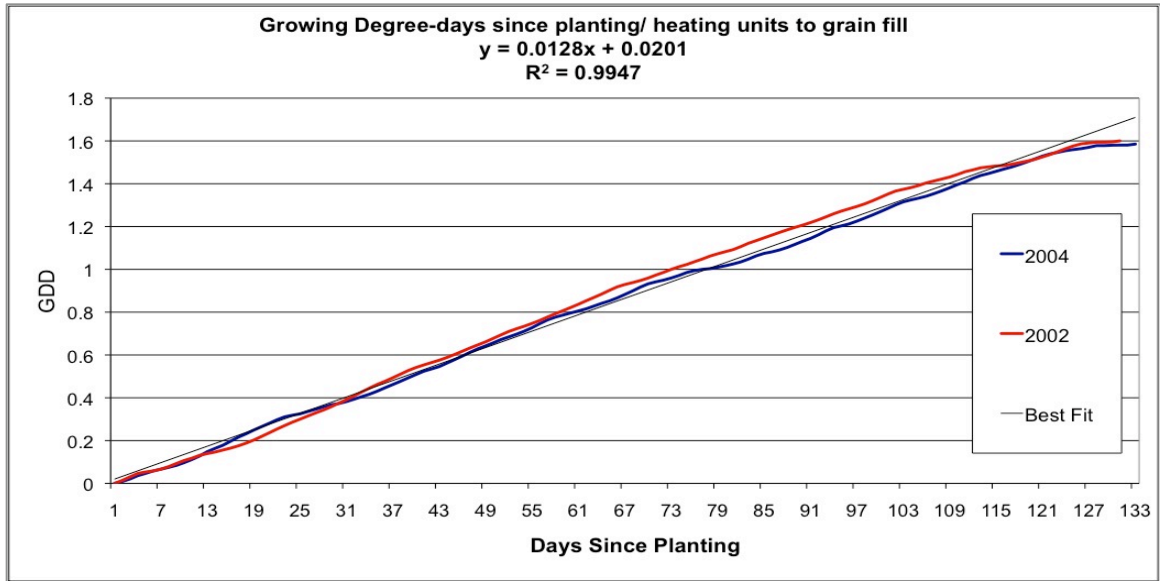


**Figure 15.** Ratio of Growing Degree-Days since planting divided by the heating units required to begin grain fill for 2002 and 2004 at the SoyFACE site.

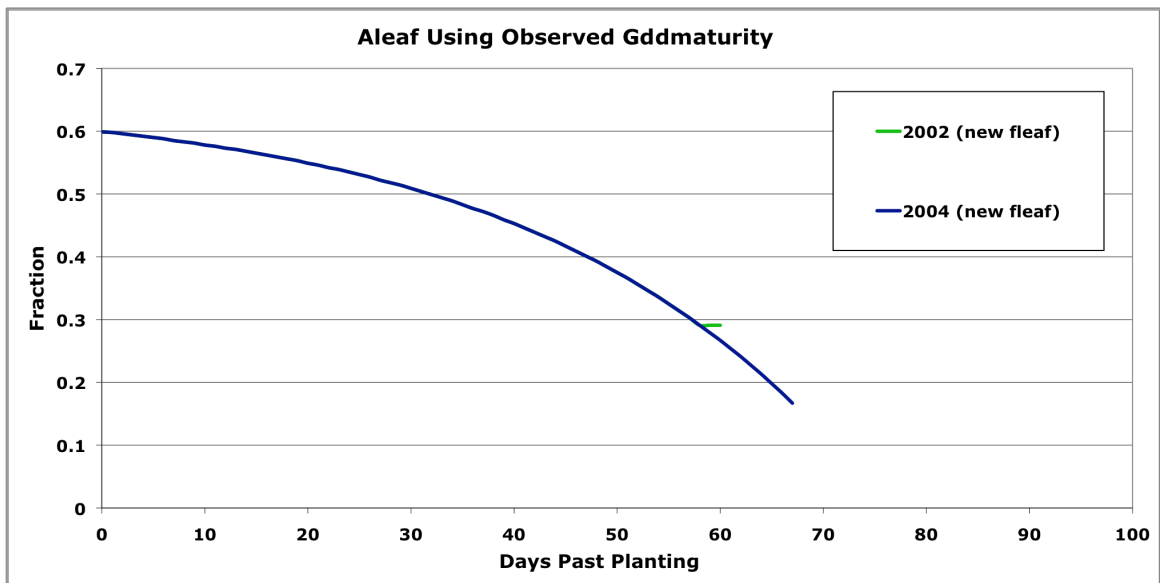


**Figure 16.** Simulated leaf fraction carbon allocation at the SoyFACE site using the observed GDD to maturity for 2002 and 2004. New fleaf is the new functions developed and old fleaf is using the old functions but using the observed GDD to maturity.



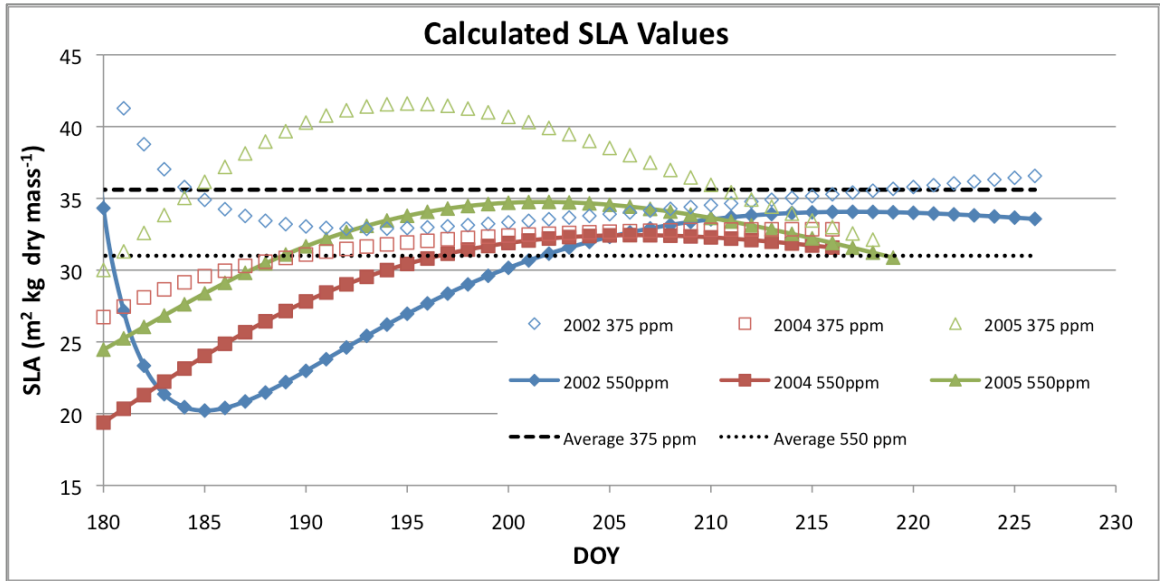


**Figure 17.** Calculated specific leaf area index (SLA) values using observed leaf dry mass and observed leaf area index measurements from the SoyFACE site. Only years 2002, 2004 and 2005 are plotted, however averaged values were calculated from all growing seasons available.

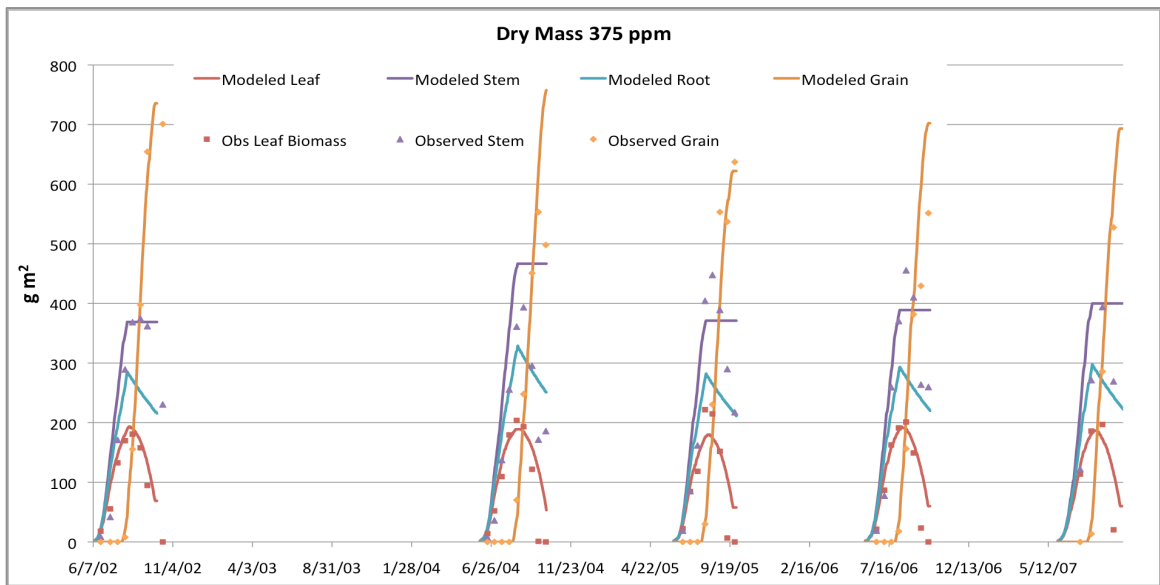


**Figure 18.** Time series of model and observed dry mass values at the SoyFACE site for ambient conditions (2002-07). Data from 2003 were excluded due to crop damage from a hail storm.

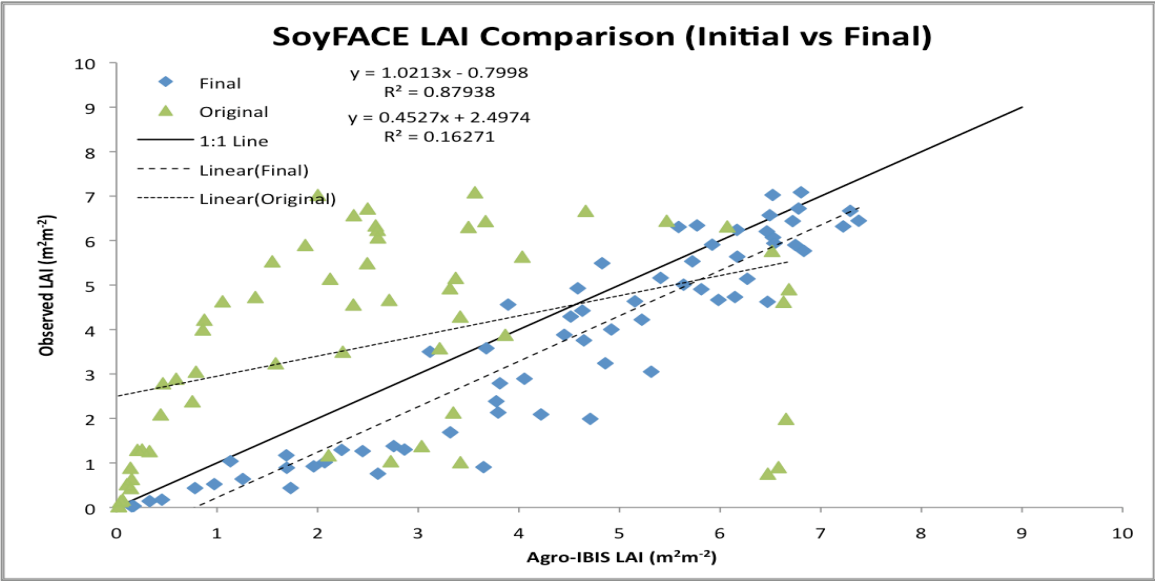


**Figure 19.** SoyFACE LAI comparison showing the model’s performance prior to and after modifications (2002 and 2004 – 2007).

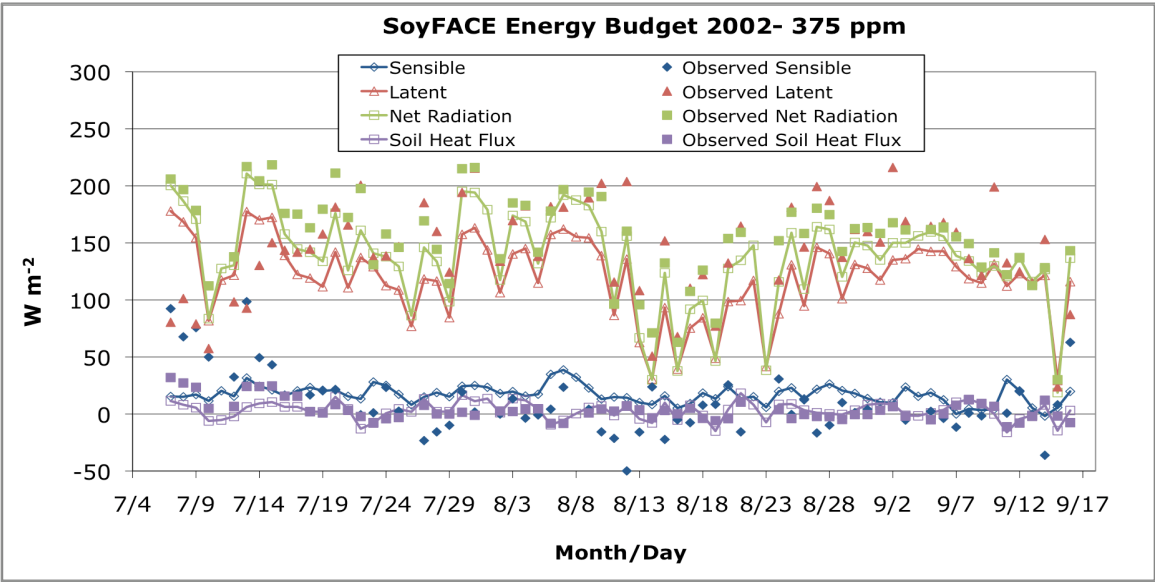


**Figure 20.** Time series of average daily values of the surface energy budget at ambient conditions at the SoyFACE site (2002).

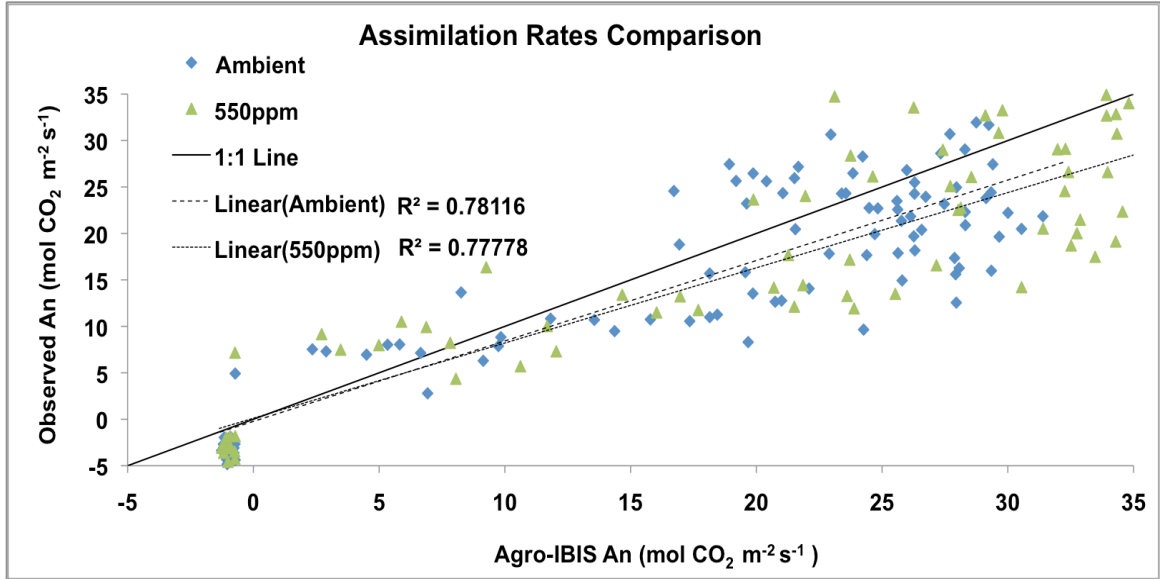


**Figure 21.** Scatter plot of observed versus simulated assimilation rates for ambient and elevated conditions for select days (2002-2004, and 2007) at the SoyFACE site.

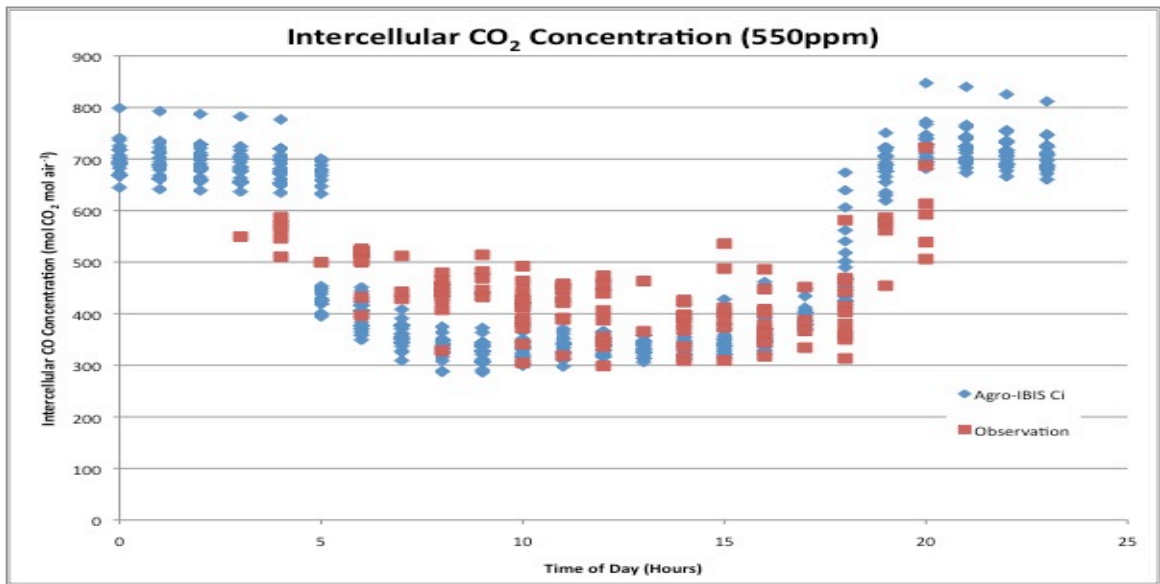


**Figure 22.** Observed and simulated intercellular CO<sub>2</sub> concentration at elevated conditions (2002-2004, and 2007) at the SoyFACE site.

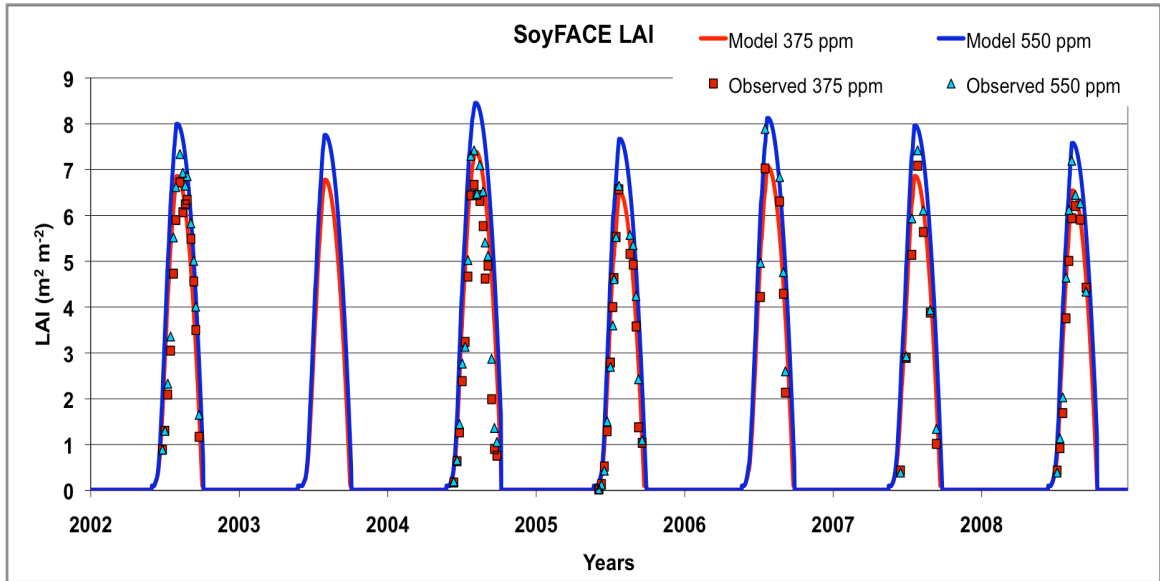


**Figure 23.** SoyFACE simulated and observed LAI at ambient and elevated conditions for 2002-2007.

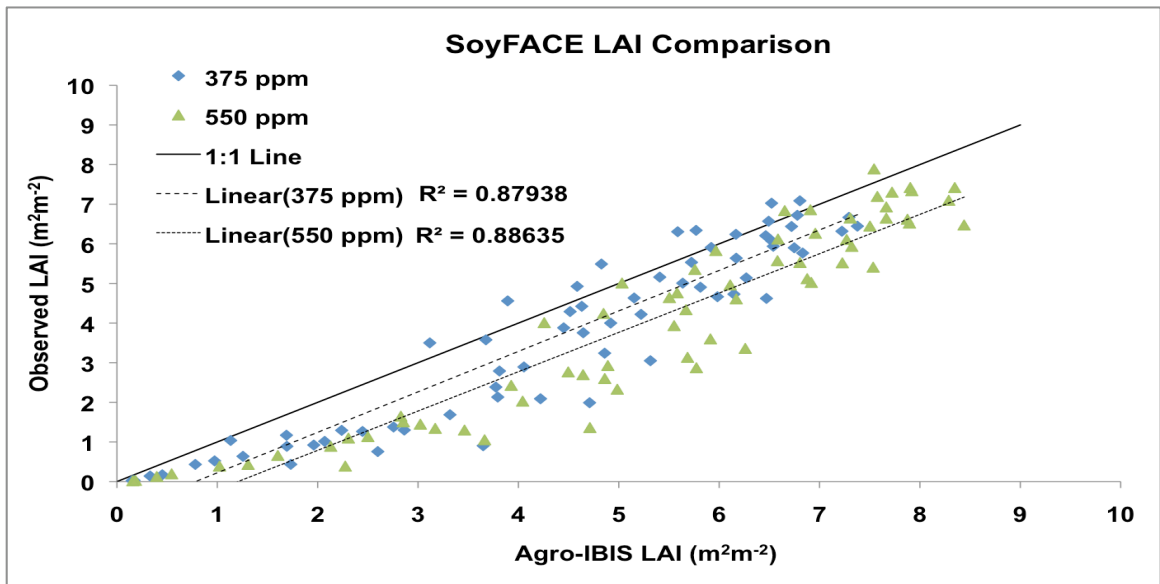


**Figure 24.** Scatter plot of observed versus simulated LAI for ambient and elevated conditions at the SoyFACE site (2002 and 2004 – 2007).

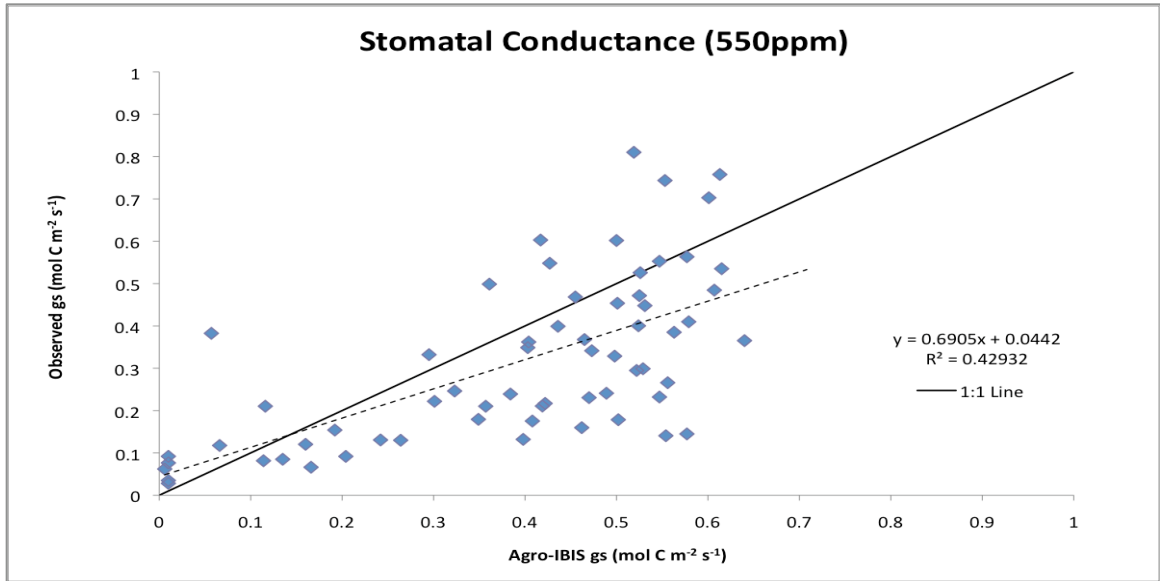


**Figure 25.** Scatter plot of observed and simulated stomatal conductance for elevated conditions (2002 – 2004, and 2007) at the SoyFACE site.

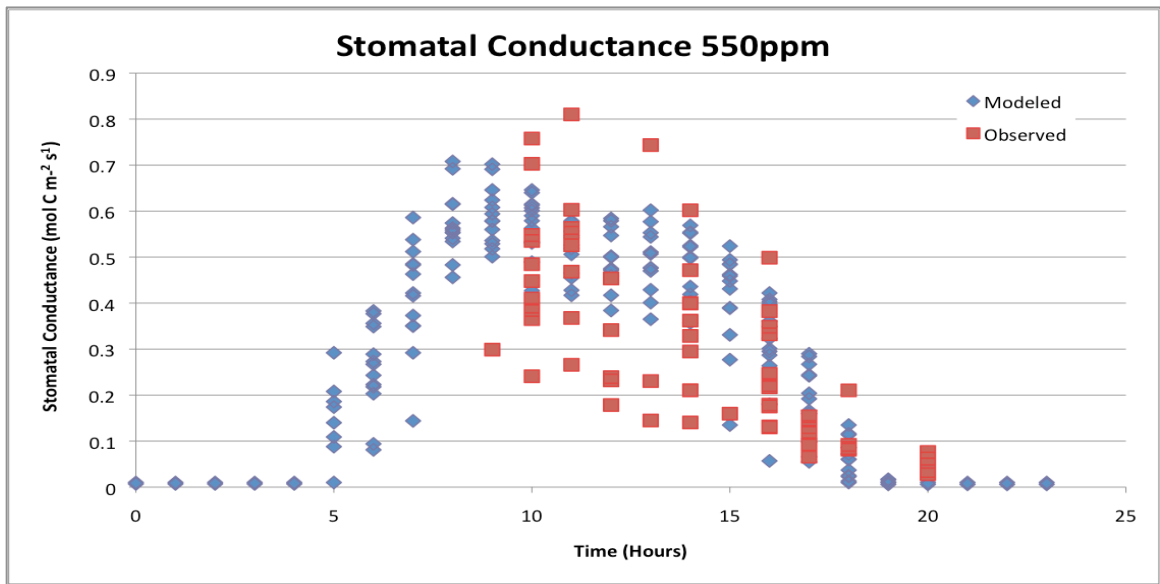


**Figure 26.** Observed and simulated stomatal conductance at elevated conditions (2002-2004, and 2007) at the SoyFACE site.

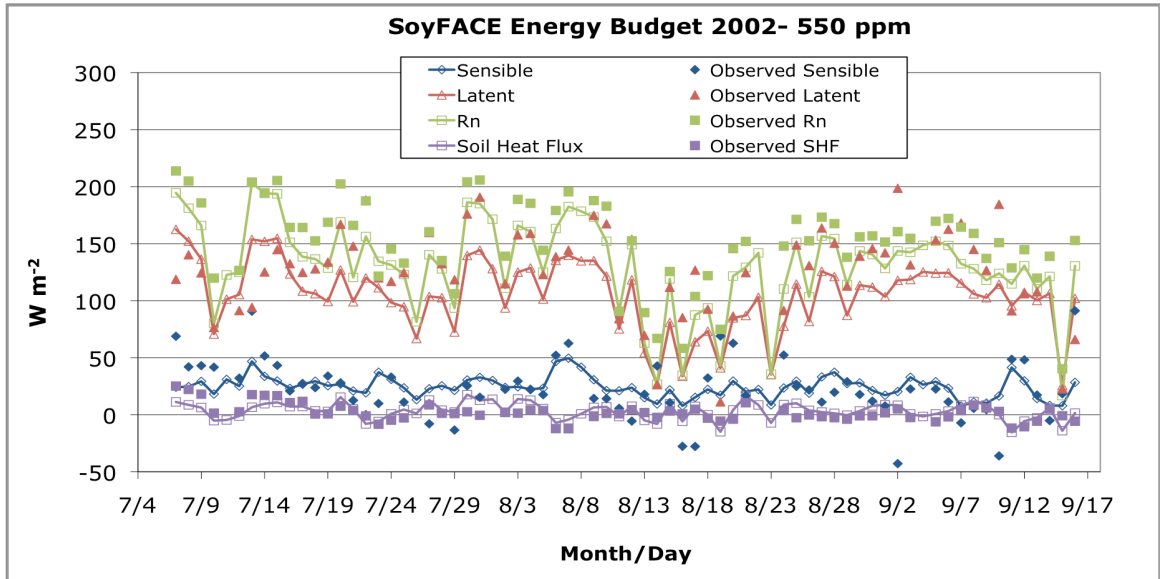


**Figure 27.** Average daily values of the surface energy budget (2002) at elevated conditions.

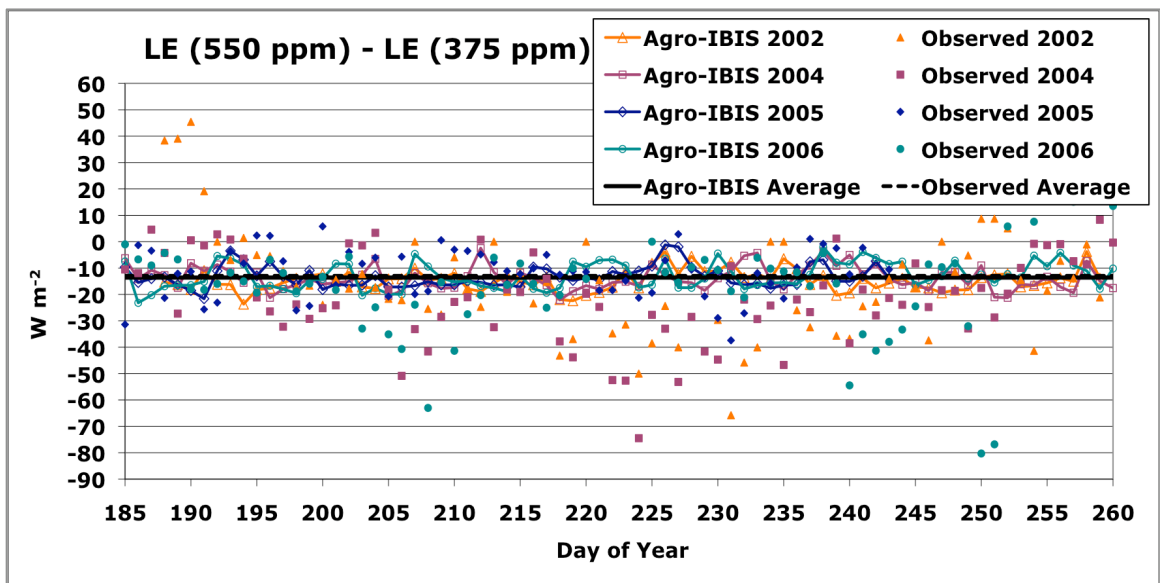


**Figure 28.** Observed and simulated change in the latent heat flux (550 ppm – 375 ppm; 2002, 2004, 2005 and 2006). Significant at ( $p < 0.05$ ).

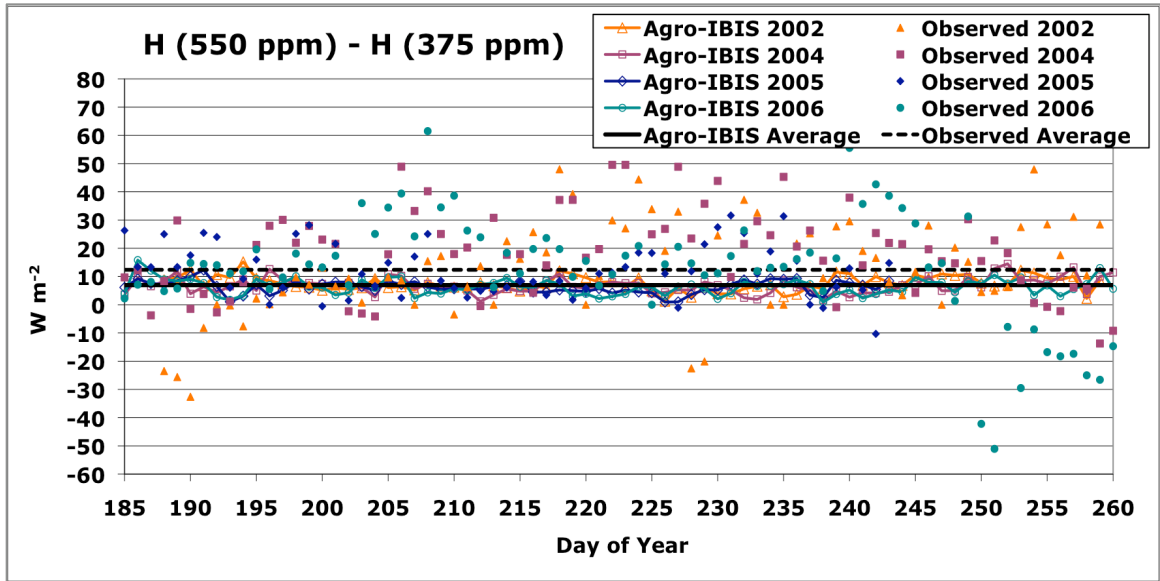


**Figure 29.** Observed and simulated change in the sensible heat flux (550 ppm – 375 ppm; 2002, 2004, 2005 and 2006) Significant at ( $p < 0.05$ ).

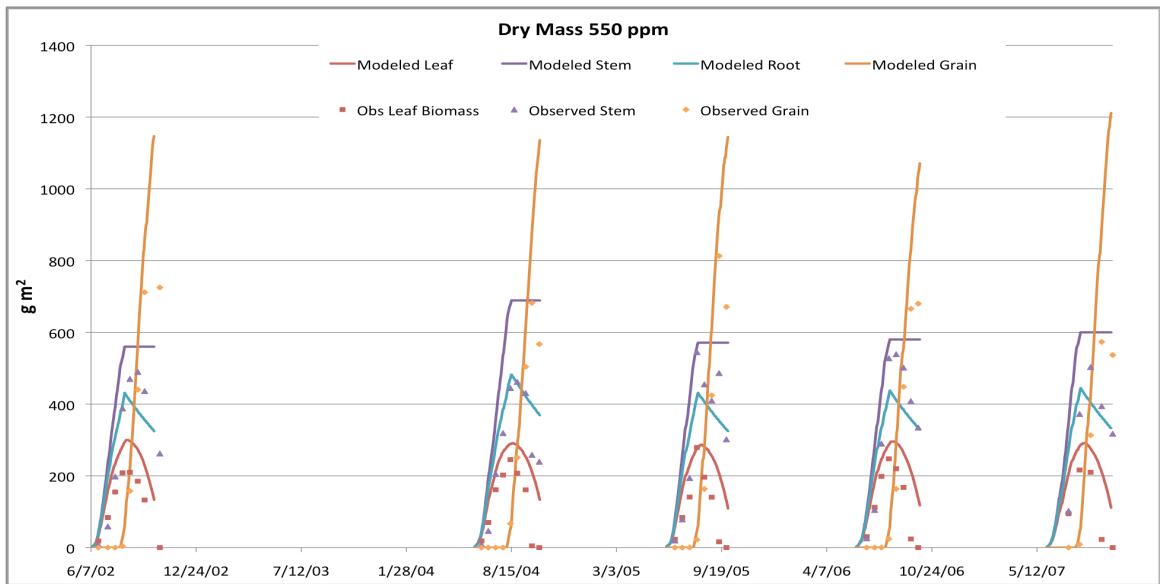


**Figure 30.** Time series of model and observed dry mass values at the SoyFACE site for elevated conditions (2002-07). Data from 2003 were excluded due to crop damage from a hail storm.

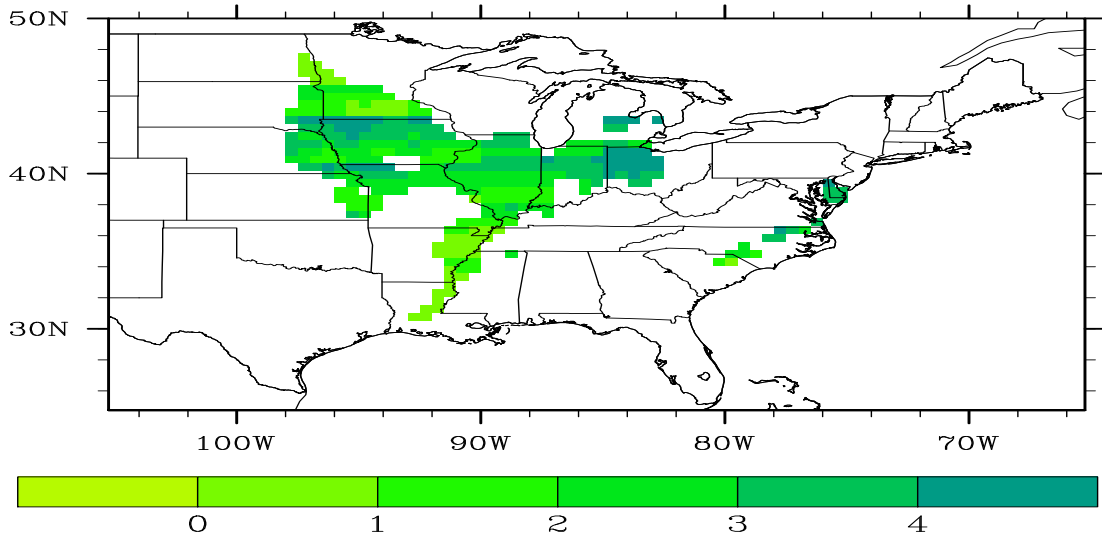


**Figure 31.** Simulated mean August LAI ( $\text{m}^2\text{m}^{-2}$ ) for 1953-2002.

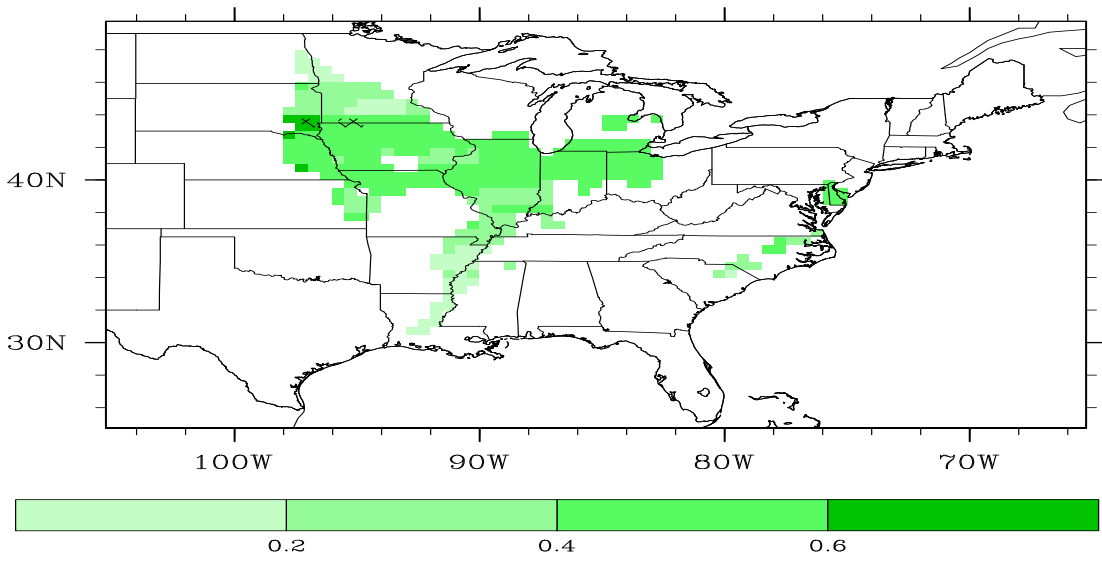


**Figure 32.** Simulated difference in mean August LAI ( $\text{m}^2\text{m}^{-2}$ ; 550 ppm – ambient) for 1953 – 2002.



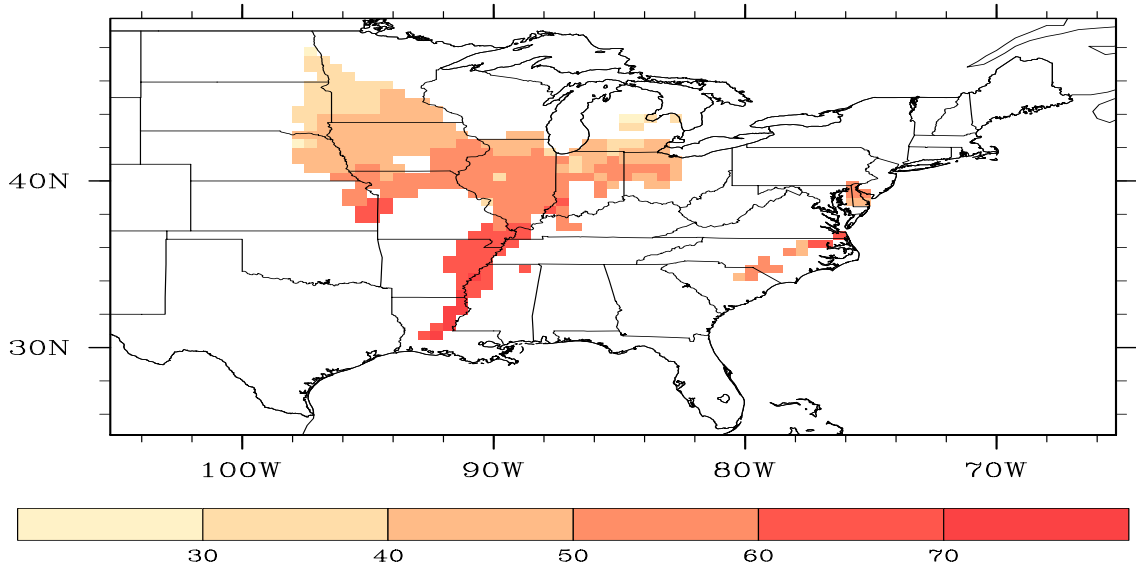


**Figure 33.** Simulated annual mean Latent Heat Flux ( $\text{W m}^{-2}$ ) for 1953-2002.

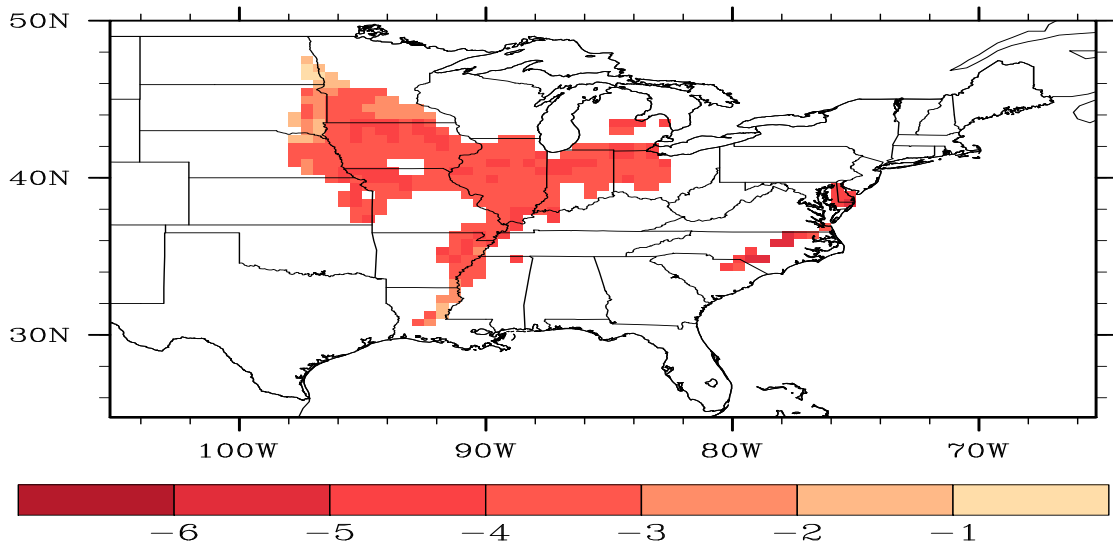


**Figure 34.** Simulated difference in annual mean latent heat flux ( $\text{W m}^{-2}$ ; 550 ppm – ambient) for 1953 – 2002.

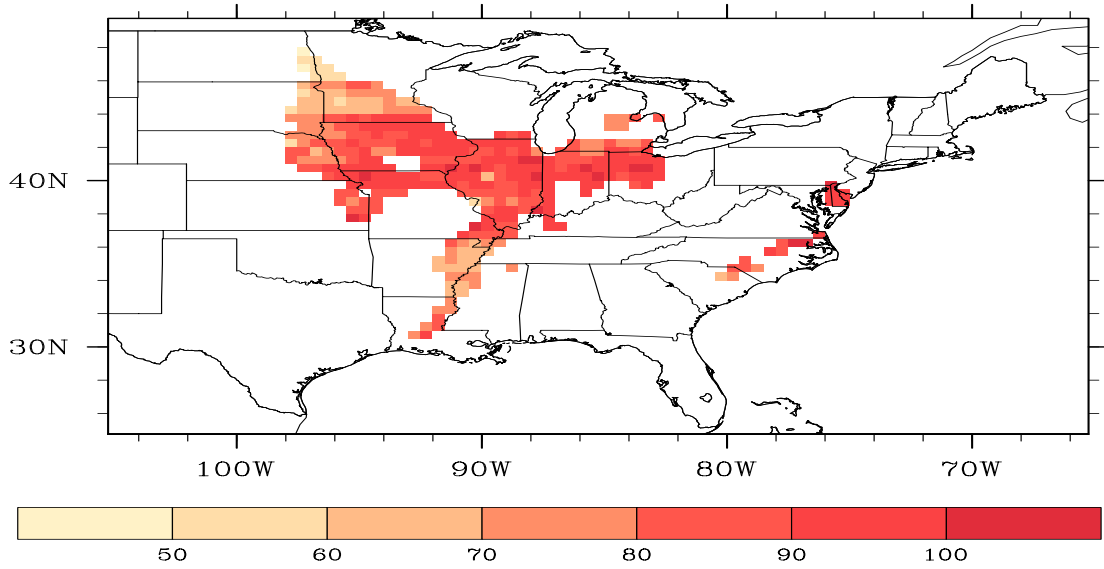


**Figure 35.** Simulated mean August Latent Heat Flux ( $\text{W m}^{-2}$ ) for 1953-2002.

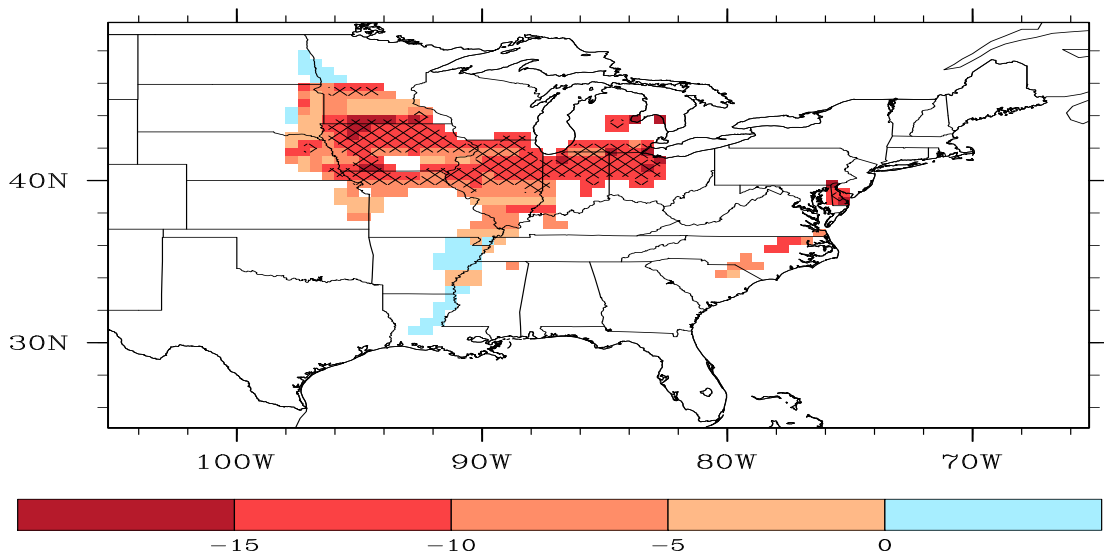


**Figure 36.** Simulated difference in mean August latent heat flux ( $\text{W m}^{-2}$ ; 550 ppm – ambient) for 1953 – 2002.

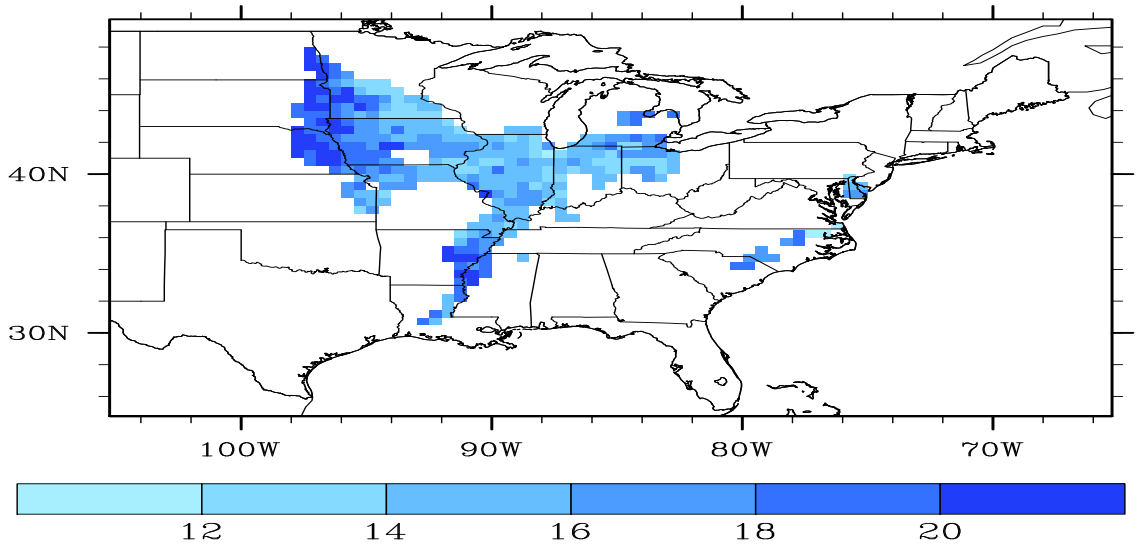


**Figure 37.** Simulated annual mean sensible heat flux ( $\text{W m}^{-2}$ ) for 1953-2002.

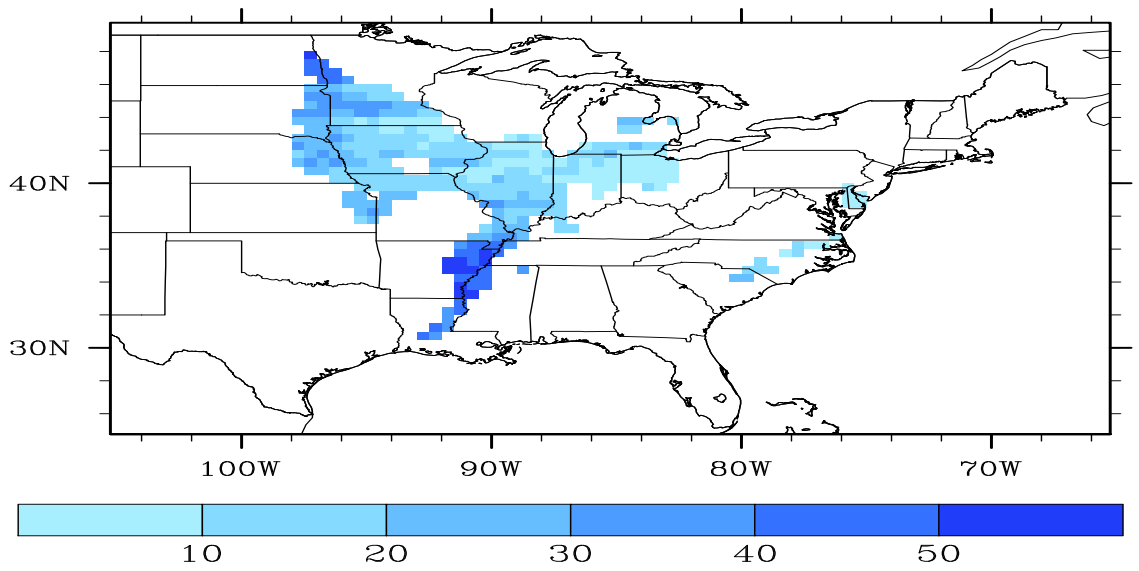


**Figure 38.** Simulated mean August sensible heat flux ( $\text{W m}^{-2}$ ) for 1953-2002.

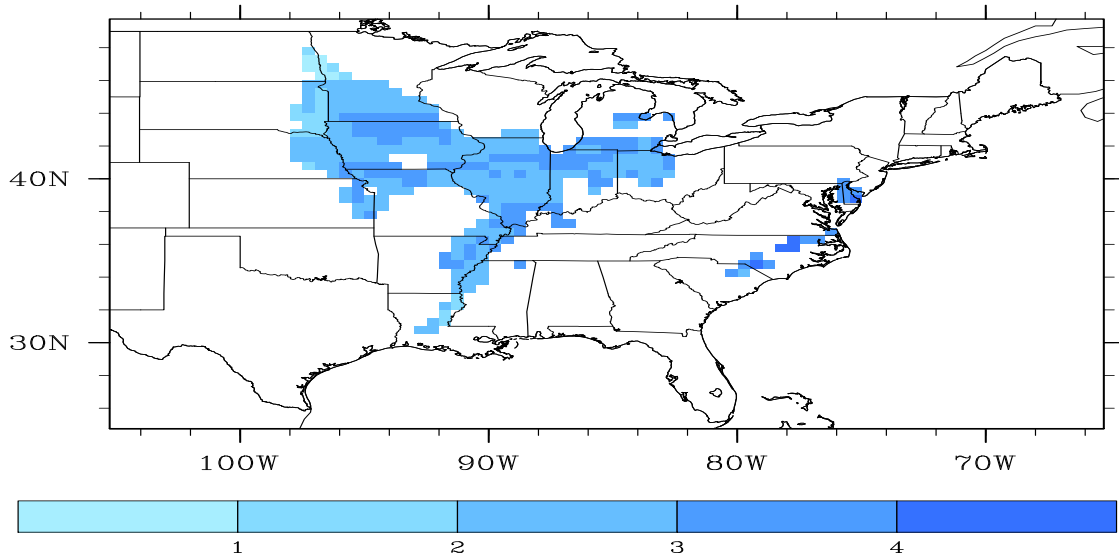


**Figure 39.** Simulated difference in annual mean sensible heat flux ( $\text{W m}^{-2}$ ; 550 ppm – ambient) for 1953 – 2002.

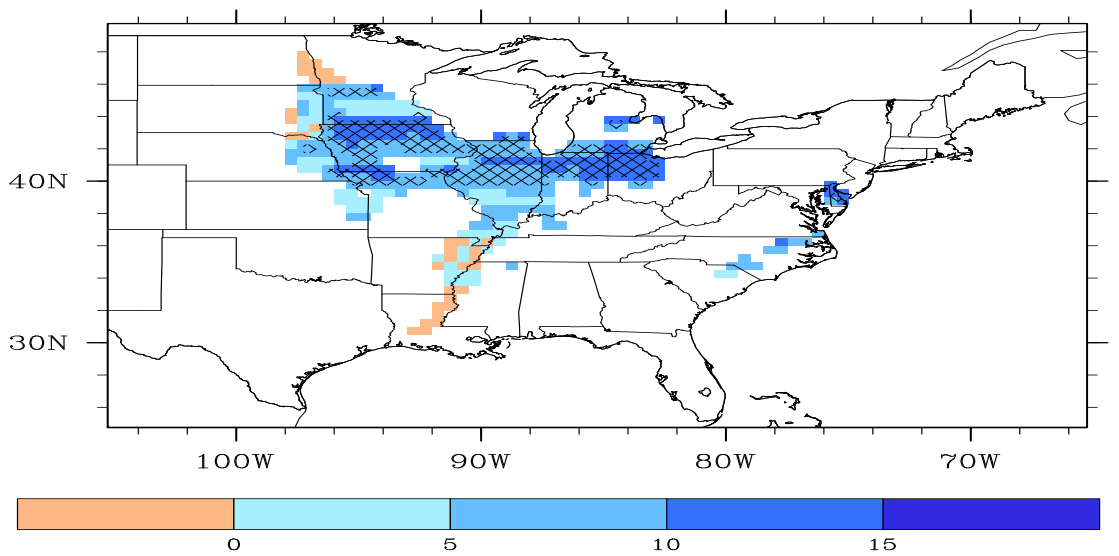


**Figure 40.** Simulated difference in mean August sensible heat flux ( $\text{W m}^{-2}$ ; 550 ppm – ambient) for 1953 – 2002.

## Bibliography

- USDA (2010). Agricultural Statistics Board, Cornell University. "Crop Production 2009 Summary."
- Ainsworth, E. A., P. A. Davey, et al. (2002). "A meta-analysis of elevated [CO<sub>2</sub>] effects on soybean (*Glycine max*) physiology, growth and yield." *Global Change Biology* **8**(8): 695-709.
- Ainsworth, E. A. and A. Rogers (2007). "The response of photosynthesis and stomatal conductance to rising [CO<sub>2</sub>]: mechanisms and environmental interactions." *Plant Cell and Environment* **30**(3): 258-270.
- Amthor, J. S. (1984). "The Role of Maintenance Respiration in Plant-Growth." *Plant Cell and Environment* **7**(8): 561-569.
- Arp, W. J., J. E. M. Van Mierlo, et al. (1998). "Interactions between elevated CO<sub>2</sub> concentration, nitrogen and water: effects on growth and water use of six perennial plant species." *Plant, Cell & Environment* **21**(1): 1-11.
- Baker, J. M. and T. J. Griffis (2005). "Examining strategies to improve the carbon balance of corn/soybean agriculture using eddy covariance and mass balance techniques." *Agricultural and Forest Meteorology* **128**(3-4): 163-177.
- Baldocchi, D. D., B. B. Hicks, et al. (1988). "Measuring Biosphere-Atmosphere Exchanges of Biologically Related Gases with Micrometeorological Methods." *Ecology* **69**(5): 1331-1340.
- Bernacchi, C. J., B. A. Kimball, et al. (2007). "Decreases in stomatal conductance of soybean under open-air elevation of [CO<sub>2</sub>] are closely coupled with decreases in ecosystem evapotranspiration." *Plant Physiology* **143**(1): 134-144.
- Bernacchi, C. J., A. D. B. Leakey, et al. (2006). "Hourly and seasonal variation in photosynthesis and stomatal conductance of soybean grown at future CO<sub>2</sub> and ozone concentrations for 3 years under fully open-air field conditions." *Plant Cell and Environment* **29**(11): 2077-2090.
- Bernacchi, C. J., E. L. Singsaas, et al. (2001). "Improved temperature response functions for models of Rubisco-limited photosynthesis." *Plant, Cell & Environment* **24**(2): 253-259.
- Campbell, G. S. and J. M. Norman (1998). *An Introduction to Environmental Biophysics*, Springer-Verlag, New York.
- Collatz, G. J., J. T. Ball, et al. (1991). "Physiological and Environmental-Regulation of Stomatal Conductance, Photosynthesis and Transpiration - a Model That Includes a Lamina Boundary-Layer." *Agricultural and Forest Meteorology* **54**(2-4): 107-136.
- Cramer, W., A. Bondeau, et al. (2001). "Global response of terrestrial ecosystem structure and function to CO<sub>2</sub> and climate change: results from six dynamic global vegetation models." *Global Change Biology* **7**(4): 357-373.
- Dermody, O., S. P. Long, et al. (2006). "How does elevated CO<sub>2</sub> or ozone affect the leaf-area index of soybean when applied independently?" *New Phytologist* **169**(1): 145-155.

- Donner, S. D., M. T. Coe, et al. (2002). "Modeling the impact of hydrological changes on nitrate transport in the Mississippi River Basin from 1955 to 1994." Global Biogeochemical Cycles **16**(3): -.
- Donner, S. D. and C. J. Kucharik (2003). "Evaluating the impacts of land management and climate variability on crop production and nitrate export across the Upper Mississippi Basin." Global Biogeochemical Cycles **17**(3): -.
- Donner, S. D. and C. J. Kucharik (2008). "Corn-based ethanol production compromises goal of reducing nitrogen export by the Mississippi River." Proceedings of the National Academy of Sciences of the United States of America **105**(11): 4513-4518.
- Farquhar, G. D., S. V. Caemmerer, et al. (1980). "A Biochemical-Model of Photosynthetic Co<sub>2</sub> Assimilation in Leaves of C-3 Species." Planta **149**(1): 78-90.
- Field, C., C. Lund, et al. (1997). "CO<sub>2</sub> effects on the water budget of grassland microcosm communities." Global Change Biology **3**(3): 197-206.
- Foley, J. A., I. C. Prentice, et al. (1996). "An integrated biosphere model of land surface processes, terrestrial carbon balance, and vegetation dynamics." Global Biogeochemical Cycles **10**(4): 603-628.
- Hamilton, J., O. Dermody, et al. (2005). "Anthropogenic changes in tropospheric composition increase susceptibility of soybean to insect herbivory." Environmental Entomology **34**: 479-485.
- Hickman, G. C., A. Vanloocke, et al. (2010). "A comparison of canopy evapotranspiration for maize and two perennial grasses identified as potential bioenergy crops." Global Change Biology Bioenergy **2**(4): 157-168.
- Kalnay, E., M. Kanamitsu, et al. (1996). "The NCEP/NCAR 40-year reanalysis project." Bulletin of the American Meteorological Society **77**(3): 437-471.
- Kimball, B. A., J. R. Mauney, et al. (1993). "Effects of Increasing Atmospheric Co<sub>2</sub> on Vegetation." Vegetatio **104**: 65-75.
- Kistler, R., E. Kalnay, et al. (2001). "The NCEP-NCAR 50-year reanalysis: Monthly means CD-ROM and documentation." Bulletin of the American Meteorological Society **82**(2): 247-267.
- Kucharik, C. J. (2003). "Evaluation of a Process-Based Agro-Ecosystem Model (Agro-IBIS) across the US Corn Belt: Simulations of the Interannual Variability in Maize Yield." Earth Interactions **7**: -.
- Kucharik, C. J. and K. R. Brye (2003). "Integrated Biosphere Simulator (IBIS) yield and nitrate loss predictions for Wisconsin maize receiving varied amounts of nitrogen fertilizer." Journal of Environmental Quality **32**(1): 247-268.
- Kucharik, C. J., J. A. Foley, et al. (2000). "Testing the performance of a Dynamic Global Ecosystem Model: Water balance, carbon balance, and vegetation structure." Global Biogeochemical Cycles **14**(3): 795-825.
- Kucharik, C. J. and T. E. Twine (2007). "Residue, respiration, and residuals: Evaluation of a dynamic agroecosystem model using eddy flux measurements and biometric data." Agricultural and Forest Meteorology **146**(3-4): 134-158.
- Leavitt, S. W., E. A. Paul, et al. (1996). "Carbon isotopes and carbon turnover in cotton and wheat FACE experiments." Plant and Soil **187**(2): 147-155.

- Long, S. P., E. A. Ainsworth, et al. (2006). "Food for thought: Lower-than-expected crop yield stimulation with rising CO<sub>2</sub> concentrations." Science **312**(5782): 1918-1921.
- Long, S. P., E. A. Ainsworth, et al. (2004). "Rising atmospheric carbon dioxide: Plants face the future." Annual Review of Plant Biology **55**: 591-628.
- Loveland, T. R. and A. S. Belward (1997). "The IGBP-DIS global 1 km land cover data set, DISCover: first results." International Journal of Remote Sensing **18**(15): 3291-3295.
- McMurtrie, R. E., R. J. Norby, et al. (2008). "Why is plant-growth response to elevated CO<sub>2</sub> amplified when water is limiting, but reduced when nitrogen is limiting? A growth-optimisation hypothesis." Functional Plant Biology **35**(6): 521-534.
- Mitchell, T. D. and P. D. Jones (2005). "An improved method of constructing a database of monthly climate observations and associated high-resolution grids." International Journal of Climatology **25**(6): 693-712.
- Morgan, P. B., G. A. Bollero, et al. (2005). "Smaller than predicted increase in aboveground net primary production and yield of field-grown soybean under fully open-air [CO<sub>2</sub>] elevation." Global Change Biology **11**(10): 1856-1865.
- New, M., M. Hulme, et al. (1999). "Representing twentieth-century space-time climate variability. Part I: Development of a 1961-90 mean monthly terrestrial climatology." Journal of Climate **12**(3): 829-856.
- Pacala, S. and R. Socolow (2004). "Stabilization wedges: Solving the climate problem for the next 50 years with current technologies." Science **305**(5686): 968-972.
- Pollard, D. and S. L. Thompson (1995). "Use of a Land-Surface-Transfer Scheme (Lsx) in a Global Climate Model - the Response to Doubling Stomatal-Resistance." Global and Planetary Change **10**(1-4): 129-161.
- Ramankutty, N., C. Delire, et al. (2006). "Feedbacks between agriculture and climate: An illustration of the potential unintended consequences of human land use activities." Global and Planetary Change **54**(1-2): 79-93.
- Ramankutty, N. and J. A. Foley (1998). "Characterizing patterns of global land use: An analysis of global croplands data." Global Biogeochemical Cycles **12**(4): 667-685.
- Rogers, A., D. J. Allen, et al. (2004). "Leaf photosynthesis and carbohydrate dynamics of soybeans grown throughout their life-cycle under Free-Air Carbon dioxide Enrichment." Plant Cell and Environment **27**(4): 449-458.
- Rosenzweig, C., and M.L. Parry (1994). "Potential impact of climate change on world food supply." Nature **367**: 133-138.
- Ryan, M. G. (1991). "Effects of Climate Change on Plant Respiration." Ecological Applications **1**(2): 157-167.
- Sellers, P. J., R. E. Dickinson, et al. (1997). "Modeling the exchanges of energy, water, and carbon between continents and the atmosphere." Science **275**(5299): 502-509.
- Setiyono, T. D., A. Weiss, et al. (2007). "Understanding and modeling the effect of temperature and daylength on soybean phenology under high-yield conditions." Field Crops Research **100**: 257-271.
- von Caemmerer, S. and R. T. Furbank (2003). "The C-4 pathway: an efficient CO<sub>2</sub> pump." Photosynthesis Research **77**(2-3): 191-207.

Zhang, L. X., Kyei-Boahen, S., Zhang, J., Zhang, M. H., Freeland, T. B., Watson, C. E., Jr., and Liu, X. M. (2007). "Modifications of optimum adaptation zones for soybean maturity groups in the USA." Crop Management **Online**.



## Appendix I.

### Rosemount and Bondville Evaluation

Meteorological data for the Rosemount and Bondville sites were collected from the Ameriflux website <ftp://cdiac.ornl.gov/pub/ameriflux/data/> (Table 2). Several different maturity group values were used to test the model at the Rosemount and Bondville sites. A Flanagan soil profile was used to run the model at the Bondville sites. For the Rosemount site a silt loam soil texture was used for the upper 2 meters and sand from 2.0-2.5 m. Rosemount (2004-2006) model simulations were run at an hourly time step, and Bondville (1996-2006) model simulations were run at a half-hourly time step. For the Rosemount runs, corn was simulated for 1889-2002, and soybean for 2003-2006. For the Bondville runs, corn was simulated for 1889-1999, and soybean for 2000-2007.

### Bondville, IL

The Bondville, Illinois (40°0'22''N, 88°17'25''W, 219 m a.s.l.) site (hereafter referred to as Bondville) is part of the Ameriflux network and global FLUXNET network of micrometeorological tower measurements of terrestrial carbon fluxes (<http://www.fluxnet.ornl.gov>). The Bondville site is located in Champaign, Illinois and is approximately 1.6 kilometers from the SoyFACE facility. The site contains two fields that alternate a corn and soybean rotation to provide measurements over both crops each year. The first field was established in 1996 and the companion site was established in 2004. The fields are continuous no-till and contain three soil series: Dana (Fine-silty,

mixed, mesic, Typic Argiudolls), Flanagan (Fine, montmorillonitic, mesic, Aquic Argiudolls), and Drummer (Fine-silty, mixed, mesic, Typic Haplaquolls) according to the USDA Natural Resources Conservation Service; <http://soils.usda.gov/>.

Continuous observations of ecosystem-level exchanges of CO<sub>2</sub>, energy and momentum fluxes are collected at all Ameriflux sites using an eddy covariance method. The eddy covariance method is a statistical method that analyzes high-frequency wind and scalar atmospheric data series to obtain fluxes of CO<sub>2</sub>, energy and momentum (Baldocchi et al., 1988). Observations of LAI were periodically collected throughout the growing season with 13 observations in 2002, 11 in 2003, 15 in 2004, 12 in 2005, and 7 in 2006.

### **Rosemount, MN**

The Rosemount, Minnesota (44°43'18''N, 94°54'39''W, 259.7 m a.s.l.) site (hereafter referred to as Rosemount) is also part of the Ameriflux regional network and global FLUXNET network. It is located at the University of Minnesota's Rosemount Research and Outreach Center, approximately 25 km south of St. Paul, MN. Before being cultivated the site was an upland prairie consisting mainly of C3 and C4 grasses. The site was first tilled in 1879 and wheat was planted. Corn became the dominant crop sometime in the 20<sup>th</sup> century and from 1998-2001 corn was planted annually. Starting in 2002 a corn-soybean annual rotation was implemented (Baker and Griffis, 2005). The soil texture is silt loam in the first 2 meters with a sand-gravel under layer. NEE, energy and momentum fluxes are measured using the eddy covariance method. LAI values are collected periodically throughout the growing season with 13 measurements collected in 2004 and 14 in 2006.

## Results of the Model Evaluation at Ambient [CO<sub>2</sub>]: Ameriflux Sites

### 4.3.1 LAI

For the Rosemount and Bondville sites, the simulation of three maturity groups shows the model's ability to capture differences in the hybrids. Rosemount, MN falls into the maturity group 1 region defined by Zhang et al. (2007). However, when the maturity group is set to 1 in Agro-IBIS, soybean matures too quickly and reaches its peak LAI too early in 2004 and 2006 (Fig. A1.1). Maturity group 1 reaches its peak LAI 13- 15 days before the maturity group 2 and about 30 days before observations. Maturity group 3 results in an LAI that peaks within two to three days of observations and compares well in magnitude with 6.65 and 6.96 m<sup>2</sup> m<sup>-2</sup> (simulated and observed, respectively). Agro-IBIS simulates a peak LAI value of 3.61 m<sup>2</sup> m<sup>-2</sup> in 2006, which was well below the observed value of 8.16 m<sup>2</sup> m<sup>-2</sup>. The model overestimates the impacts of the precipitation decrease during 2006, which experienced 49.72 mm less rainfall during the first 15 days of June as compared to 2004, which saw 79.53 mm during the same period.

The use of maturity group 3 provides the best comparison with observations for the Bondville site. Maturity group 2 limits the leaf development and maturity group 4 reaches a slightly higher peak LAI for most years (Fig. A1.2). Using the maturity group 3, the model did well at both the timing and magnitude of leaf development in 2003 and 2005 but in 2004 the model oversimulated the peak by 1.42 m<sup>2</sup> m<sup>-2</sup>. This overestimation in 2004 also occurred at the SoyFACE site, which has virtually the same weather given their proximity. The climate of 2004 was cooler (Fig. 13), and these lower temperatures led the model to over simulate the LAI due to the delay in the initiation of grain fill.

Overall the model performed well for the three sites at ambient [CO<sub>2</sub>] concentrations. The model had a slight bias to overestimate the LAI, with an R<sup>2</sup> value for the three sites of 0.61 (Fig. A1.3).

#### 4.3.2 Net Ecosystem Exchange

At the Bondville site the model overestimates the soybean carbon sink by 222.13 g C in 2004 and 249.11 g C in 2006 (Fig. A1.4). In 2004 the model over predicted carbon sequestration in June and August and was close to observations in July, with a total overestimation of 5.68 g C day<sup>-1</sup> for these three months. During 2006 the model over predicted carbon sequestration during the growing season by 5.13 g C day<sup>-1</sup>.

Greater carbon uptake, relative to observations, over the growing season is consistent with the model's overestimation of LAI at Bondville; however, the overestimation of carbon uptake at Rosemount in 2004 (Fig. A1.5) is inconsistent with the model's underestimation of LAI. Observed values show that the Rosemount fields were a source of carbon to the atmosphere, 1.24 and 1.31 g C day<sup>-1</sup> (2004, 2006), while the model simulated a carbon sink of 6.20 g C day<sup>-1</sup> for 2004 and a source of 1.49 g C day<sup>-1</sup> for 2006, which was close to observations. For 2006 the model underestimated the NEE by 0.18 g C day<sup>-1</sup>.

The model's ability to simulate NEE is based on how well it simulates assimilation and carbon respiration rates. At the Rosemount site the observed values of LAI in 2006 were similar to values from the 2004 growing season, which received more precipitation. However, during the 2006 growing season at the Rosemount site the model underestimated the assimilation rates. This underestimation was caused by the model's sensitivity to precipitation amounts. The model reduced the assimilation during an

extended period with little precipitation at the start of the growing season. This decline in assimilation rates appears to be a limiting factor in the model that needs to be examined further.

### 4.3.3 Energy Budget

The model overestimates  $R_{\text{net}}$  during winter at the Rosemount site for 2004 and 2006 (Fig. A1.6). This overestimation of  $R_{\text{net}}$  leads to an overestimation of G, H, and LE for these months. Simulated values of  $R_{\text{net}}$  matched observations from April to November in 2004, and from April to December in 2006. Simulated  $R_{\text{net}}$  has an error of 1.0% for 2006 and an error of 21.4% for 2004 (Table A1.1). The model overestimates H in both years, especially in July and August in 2006; however, this is mostly due to overestimation during the winter months. During the growing season there was a simulated error in LE of 0.1% for 2004 and 10.5% for 2006, while H had large errors of 66.8% and 370.56% respectively. Simulated  $R_{\text{net}}$  has an error of just 3.0% during the growing season (June-August) for 2004 and an error of 10.3% in 2006. The error in H was lower during the growing season for both years with an error of 66.8% for the 2004 growing season compared to the annual error of 124.4%. This same pattern can be seen for the LE term for 2004 with an error of 0.1% during the growing season and 16.2% for the annual error (Table A1.1).

The model simulates  $R_{\text{net}}$  well at the Bondville site with an annual error of 18.7% and 13.3% (Table A1.1) for both years (Fig. A1.7). During the growing season the model simulates  $R_{\text{net}}$  with an error of only 0.7% in 2004 and 5.6% in 2006, but errors in H and LE were larger during the growing season than over the entire year. This increase in error was caused by the model's overestimation of transpiration with the large values of LAI

for both growing seasons (Fig. A1.2). Soil heat flux was underestimated during the 2004 growing season by  $25.54 \text{ MJ m}^{-2}$ , almost half the observed value. This again was due to overestimation of LAI and increased canopy cover. For the 2006 growing season the model simulated G within  $0.55 \text{ MJ m}^{-2}$ .

## TABLES A1

**Table A1.1.** Mean Annual and Summer (June-August) Errors of Surface Energy Budget terms ( $\text{MJ m}^{-2}$ ) for the Rosemount and Bondville sites. Annual  $R_{\text{net}}$  and G Errors for the Bondville site were calculated using 341 out of 366 days in 2004 and 325 of the 365 days in 2006. For the Rosemount site the annual  $R_{\text{net}}$  and G errors were calculated using all days.

Site	$R_{\text{net}}$			Sensible Heat			Latent Heat			Ground Heat		
	Observed	Model	Error (%)	Observed	Model	Error (%)	Observed	Model	Error (%)	Observed	Model	Error (%)
Rosemount, Mn; 2004	1862.34	2261.79	21.4	422.55	948.30	124.4	1419.35	1189.57	16.2	-21.69	98.01	551.8
Rosemount, Mn; 2006	2203.35	2225.21	1.0	217.08	1182.42	444.7	1068.82	919.47	14.0	-191.52	111.97	158.5
Rosemount, (Summer; 2004)	984.20	1013.85	3.0	185.99	310.31	66.8	664.86	663.79	0.1	36.51	51.75	41.8
Rosemount, (Summer; 2006)	1113.57	999.39	10.3	84.28	396.61	370.56	640.38	573.21	10.5	57.89	42.04	27.4
Bondville, Il; 2004	2187.66	2597.62	18.7	765.20	1018.15	33.1	1540.14	1838.06	19.3	37.38	79.88	53.2
Bondville, Il; 2006	2552.57	2186.15	13.3	643.22	791.28	23.0	1654.38	1700.41	2.8	-83.19	42.05	150.5
Bondville (Summer; 2004)	996.80	1004.20	0.7	141.11	222.07	57.4	705.30	924.41	31.1	61.12	35.58	41.8
Bondville (Summer; 2006)	919.22	970.59	5.6	127.13	165.10	29.9	776.61	865.83	11.5	40.51	39.96	1.3

## FIGURES A1

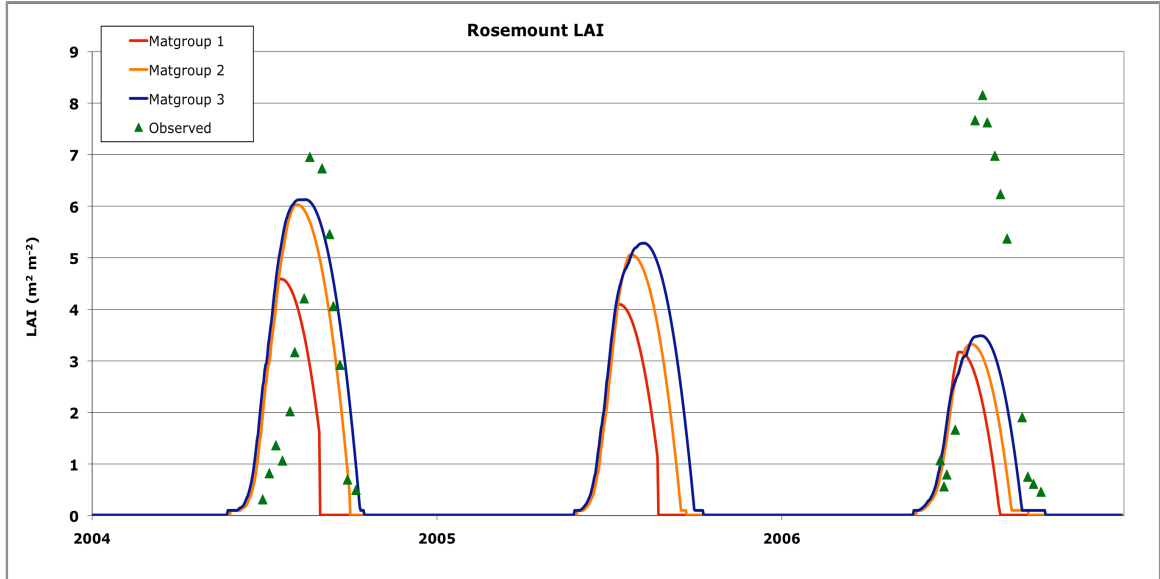


**Figure A1.1.** Plot of simulated LAI for Rosemount MN from 2004 to 2006. Three different maturity groups were simulated to test the maturity group functions.

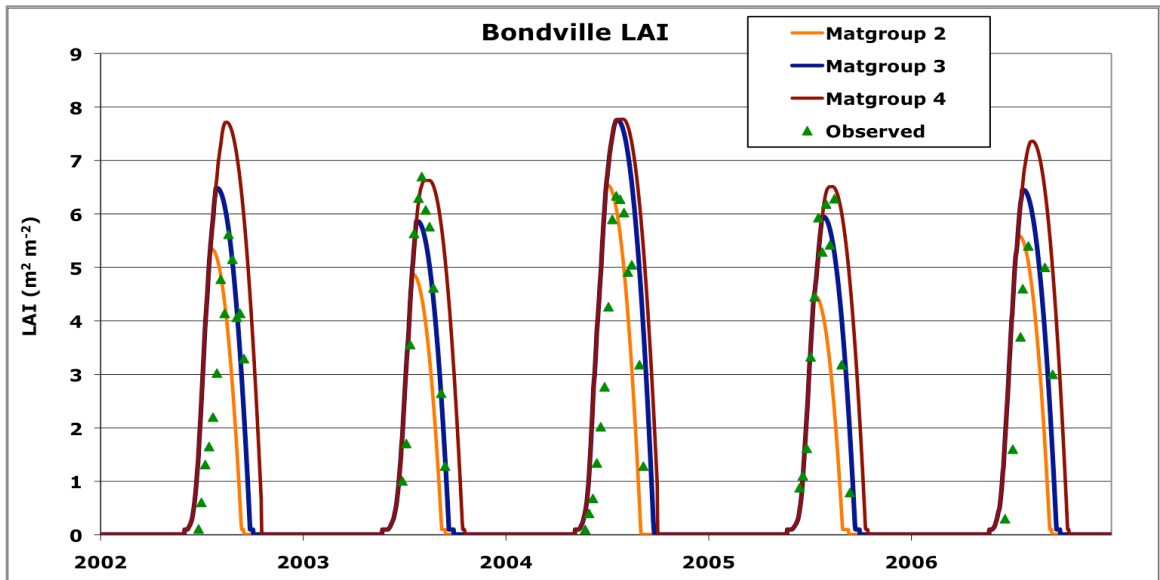


**Figure A1.2.** Simulated LAI for Bondville IL from 2002 to 2006. Three maturity groups were simulated to test the maturity group functions.



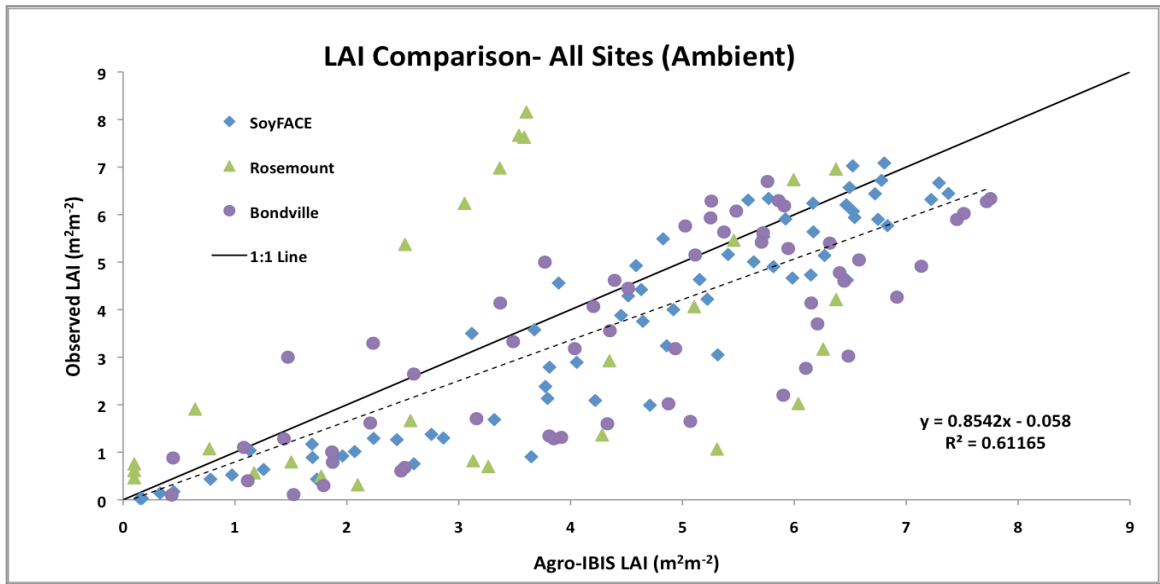


**Figure A1.3.** Scatter plot of observed versus simulated LAI for all three sites (SoyFACE – 2002 and 2004 to 2007; Rosemount – 2004 to 2006; Bondville – 2002 to 2006).

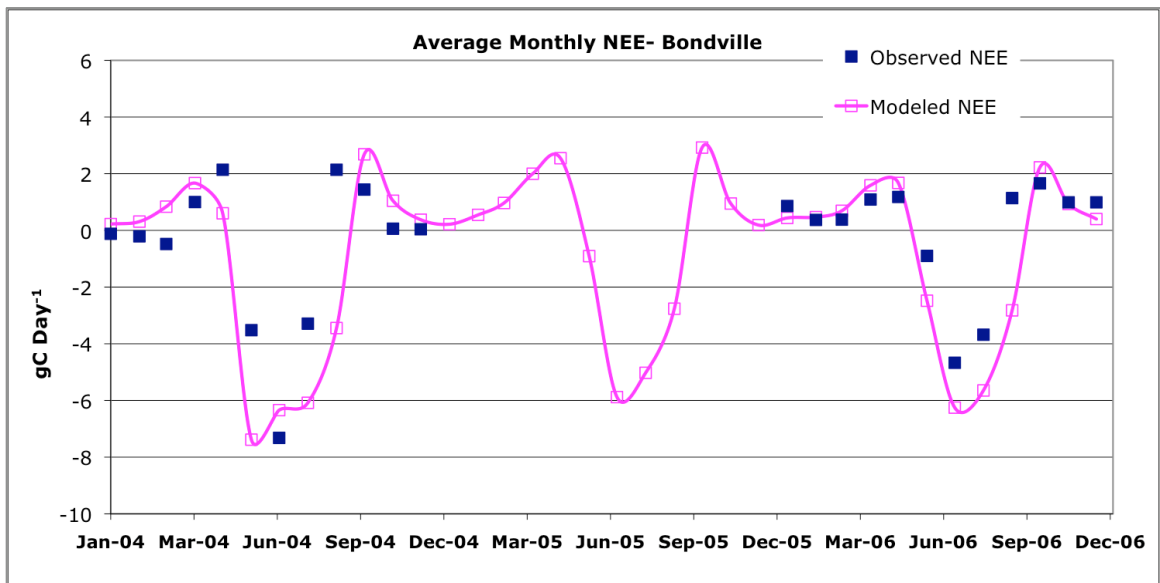


**Figure A1.4.** Average monthly NEE for the Bondville IL site for 2004-2006.

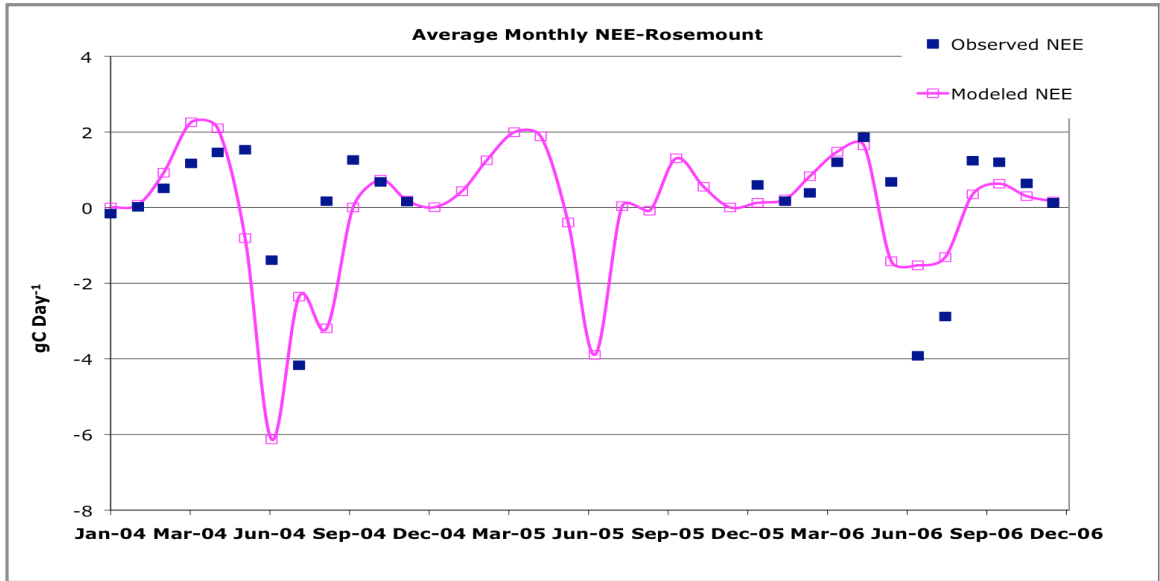


**Figure A1.5.** Average monthly NEE for Rosemount MN for 2004-2006.

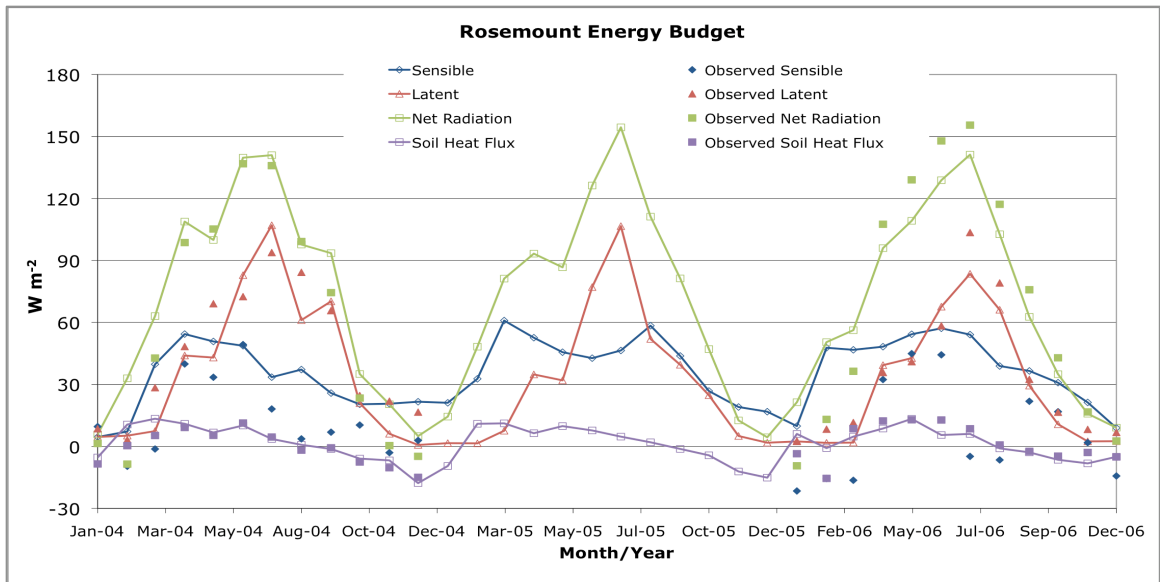


**Figure A1.6.** Time series of the averaged monthly surface energy budget (2004 – 2006) for the Rosemount MN Site.

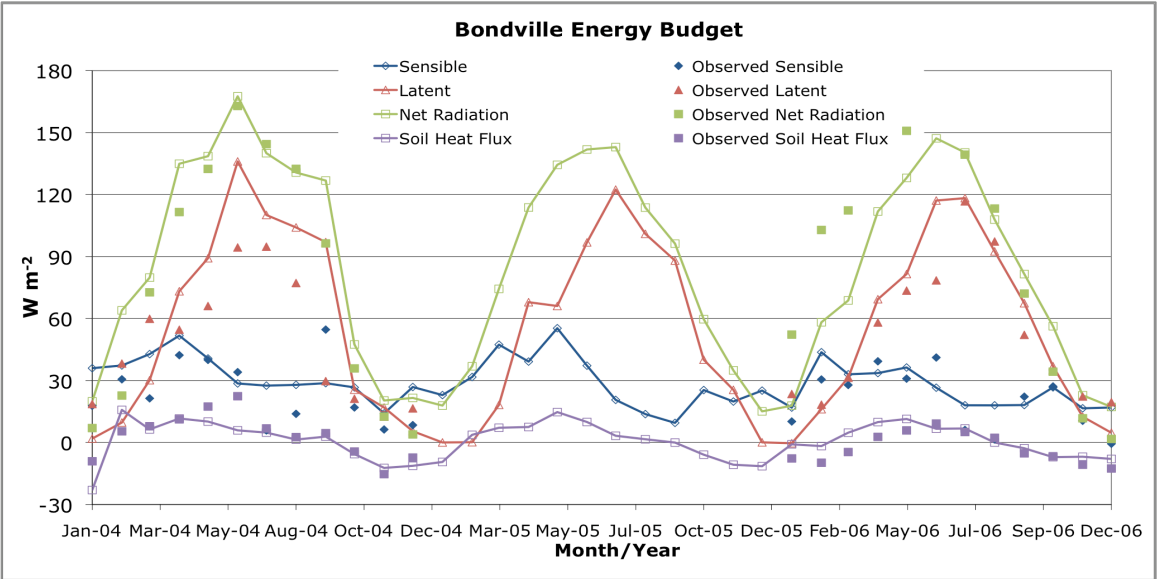


**Figure A1.7.** Time series of the averaged monthly surface energy budget (2004 – 2006) for the Bondville IL Site. Observations for the months of April and June are not shown because of many missing data points in the net radiation observations.

## Appendix II.

### Soil Carbon Simulations

The landscape of the Midwest U.S. has undergone significant changes during the last 150 years as the landscape was converted from native prairie to agricultural lands. These changes in the land cover have led to changes in assimilation rates because of the growth of different plant species as well as the introduction of fertilizer. The assimilation rates affect the amount of carbon that the crop deposits in the soil through litter return, root turnover and other more recalcitrant carbon sources in the soil (Kucharik et al., 2000). Dynamic vegetation models require realistic soil carbon to accurately simulate plant growth. Soil carbon takes thousands of years to reach equilibrium. For computational efficiency Agro-IBIS uses an accelerated soil carbon spin-up procedure to simulate the accumulation of carbon. The soil biogeochemistry module is called 40 times each day for the first 75 years (instead of performing just one execution per day). During years 76-140 there is a linear decrease in the degree of acceleration. By year 140 the biogeochemistry module is only called once per day.

Five different simulations were performed to test the sensitivity of the simulated soil carbon to different land use scenarios (Table A2.1). In four cases potential vegetation (Loveland and Belward, 1997; Ramankutty and Foley, 1998) was simulated for the initial spin-up period from 1750-1889 and for the fifth simulation, corn was grown for the entire period (1750-2001). Potential vegetation is the vegetation that would grow without the influence of humans. Following the initial spin-up period a conversion from a natural

ecosystem to corn (Simulation 1), a conversion to soybean (Simulation 2), and a conversion to a corn/soybean rotation (Simulation 3) were simulated. The fourth simulation is a conversion to corn but with the addition of a nitrogen stress function, which limits plant growth based on the availability of soil nitrogen. This simulation uses historic fertilizer application rates over the U.S. and allows for more realistic simulation of crop growth during this period. In all other simulations, the vegetation is assumed to have an unlimited supply of nitrogen.

### Results of Soil Carbon Simulations

Soil carbon content in the model reached values close to  $8.5 \text{ kg m}^{-2}$  by 2001 for all of the scenarios except the realistic nitrogen stress simulation (Simulation 4; Fig. A2.1). Simulation 4 resulted in a final soil carbon content value of  $7.7 \text{ kg m}^{-2}$ . Once the conversion from natural vegetation to corn occurred in 1890 the carbon pool began to decrease at a more rapid rate than the other simulations. Allowing the corn to respond to realistic nitrogen application rates led to a decline in productivity with conversion from natural vegetation, and hence less litter fall and root decomposition, which contributed to lower carbon values. The soil carbon then began to slowly decline and reached equilibrium around 1940 at  $8.6 \text{ kg m}^{-2}$ . In Simulations 2 and 3, where soybean was grown either in a rotation or every year resulted in final values of  $8.91$  and  $8.99 \text{ kg m}^{-2}$ , respectively. Simulations 1 and 5 resulted in values of  $8.64$  and  $8.66 \text{ kg m}^{-2}$  and show that the model simulates slightly higher soil carbon when soybean is grown and lower values when corn is grown without a corn/soybean rotation.

There are several different ways that the model spin-up can be performed. I have shown five different methods that could be performed with Simulation 4 being the most realistic approach. The simulation results show that the model simulates a difference in the carbon pools between corn and soybean, with the simulation of corn resulting in a lower carbon pool than the simulation of soybean.

## TABLES A2

**Table A2.1.** The descriptions of the accelerated carbon simulations.

Simulation	1750-1889	1890-2001
1	Natural Vegetation (Carbon Acceleration Procedure)	Corn
2	Natural Vegetation (Carbon Acceleration Procedure)	Soybean
3	Natural Vegetation (Carbon Acceleration Procedure)	Corn-Soybean Rotation
4	Natural Vegetation (Carbon Acceleration Procedure)	Corn (Realistic Nitrogen Stress)
5	Corn (Carbon Acceleration Procedure)	Corn

## FIGURES A2

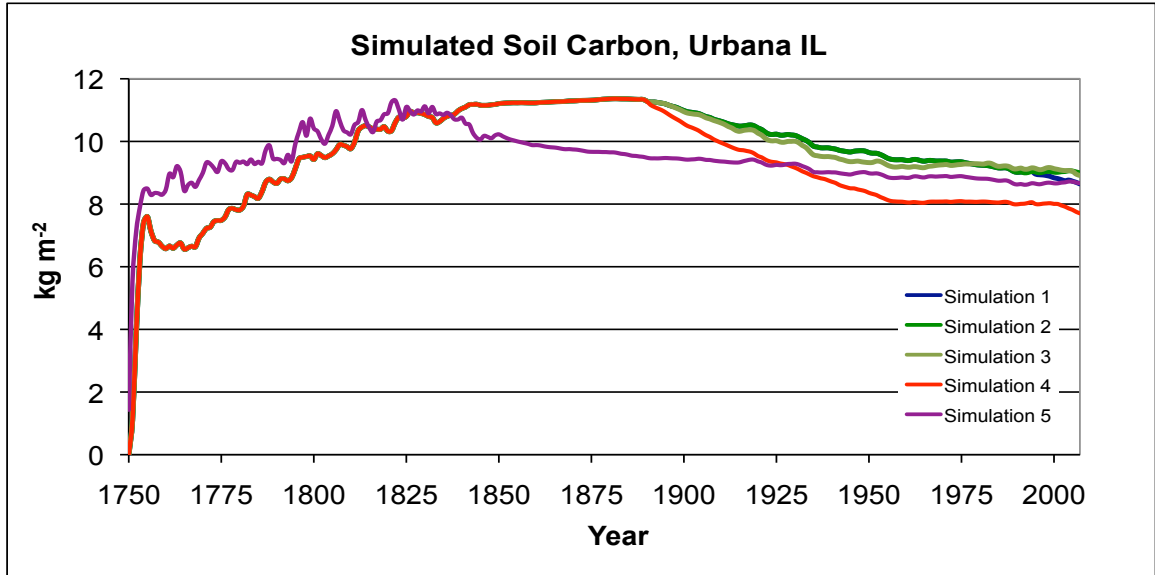


**Figure A2.1.** Simulated soil carbon at SoyFACE from 1750-2001 (Urbana, IL,; 40° 02' N, 88° 14' W, 228 m above sea level).